IEEE Access
Multidisciplinary | Rapid Review | Open Access Journal

Received November 14, 2016, accepted November 20, 2016, date of publication November 23, 2016, date of current version January 27, 2017.

*Digital Object Identifier 10.1109/ACCESS.2016.2632098*

# Throughput and Delay Analysis of Cognitive Go-Back-N Hybrid Automatic Repeat reQuest Using Discrete-Time Markov Modelling

**ATEEQ UR REHMAN, CHEN DONG, VARGHESE ANTONY THOMAS, LIE-LIANG YANG, (Fellow, IEEE), AND LAJOS HANZO, (Fellow, IEEE)**
School of Electronics and Computer Science, University of Southampton, Southampton, SO17 1BJ, U.K.

Corresponding author: L. Hanzo (lh@ecs.soton.ac.uk)

This work was supported in part by EPSRC under Project EP/Noo4558/1 and Project EP/L018659/1, in part by the European Research Council's Advanced Fellow Grant under the Beam-Me-Up Project, and in part by the Royal Society's Wolfson Research Merit Award. The work of A. U. Rehman was supported by Abdul Wali Khan University Mardan, Pakistan, under the Faculty Development Program. The research data for this paper is available at http://dx.doi.org/10.5258/SOTON/403146.

**ABSTRACT** Cognitive radio (CR) techniques have been proposed for improving the spectral efficiency by exploiting the temporarily unoccupied segments of the licensed spectrum, provided that the transmission of primary users (PUs) is not hampered. In this paper, we propose a cognitive Go-Back-N Hybrid Automatic Repeat reQuest (CGBN-HARQ) scheme that enables the cognitive user (CU) to opportunistically transmit data over a primary radio (PR) channel. Based on the sensing decisions by the CU, it decides about the availability of the PU's channel for its own transmission using the proposed CGBN-HARQ scheme. In addition, it enables the CR transmitter to receive feedback concerning the success/failure of its prior transmissions during the sensing and transmission phases of the time-slot (TS). A discrete time Markov chain model is invoked for the theoretical analysis of the proposed system, where we conceive an algorithm to generate all possible states of the CR transmitter. Both the throughput and delay of the CGBN-HARQ scheme is analyzed by deriving a range of closed-form formulas, which are validated by simulation results. The occupation of the channel by the PU and the reliability of the CU's channel significantly affect both the achievable throughput and the delay of the CGBN-HARQ scheme. Finally, our studies show that the number of packets transmitted within a TS should be adapted according to the communication channel for attaining the maximum throughput and the lowest average transmission delay.

**INDEX TERMS** Automatic repeat request, GBN-ARQ, primary radio (PR), PR channel, cognitive radio, spectrum sensing, spectrum hole, cognitive GBN-HARQ, discrete time Markov chain, throughput, delay.

## I. INTRODUCTION

The electromagnetic spectrum is a limited natural resource required for wireless communications, which became scarce due to the phenomenal growth in wireless applications in last few decades. This enormous increase in the demand for more spectrum attracted the attention of both the spectrum regulatory bodies and of the research community, since in most countries, the most valuable frequencies have already been allocated, whilst leaving no room for future applications. This then resulted in the widely recognized spectrum scarcity problem [1], [2]. Therefore, to find the root cause of the spectrum shortfall, the spectrum regulatory bodies and the research community conducted several studies during different time intervals [2]–[8]. It was found that large segments of the earmarked radio spectrum are heavily under-utilized. Explicitly, the spectrum occupancy remained between 15% and 85% [3], [4]. Following that measurements carried out at Berkley downtown indicated an approximately 30% and 0.5% occupancy for the bandwidth below 3 GHz, and in the band $3 - 6$ GHz respectively [6], [7]. These results reveal that the spectrum scarcity is not entirely a consequence of the physical shortfall, but more due to having an inefficient and inflexible SSA policy. On the other hand, the unlicensed bands, such as the Industrial, Scientific and Medical and Unlicensed National Information Infrastructure band are becoming overcrowded due to the tremendous proliferation of wireless applications, such as Wi-Fi, Blue-tooth, WiMAX and Zigbee [1], [9], [10].

The inefficient exploitation of the licensed spectrum and the congested nature of the unlicensed spectrum motivates the concept of dynamic spectrum access (DSA), which is considered to be an alternative technique of increasing the overall spectrum utilization [9]. In DSA, the unlicensed users are allowed to access the licensed spectrum for their own transmission, provided that it is temporarily unoccupied by the PUs, or if explicit permission is granted by the PUs [1], [3], [9], [11]. By doing so, the spectrum exploitation can be maximized and the PUs transmission can be protected. In 1999, Mitola and Maguire introduced the concept of Cognitive radio (CR), which has the capability of continuously monitoring and adjusting itself to the operating environment [12]. Specifically, during the monitoring phase, the CU senses the environment with the objective of detecting free slots in the licensed spectrum and then adapts some of its parameters (e.g the carrier frequency, bandwidth and modulation scheme) to reuse the available spectrum without violating the legal rights of PUs [13]. Moreover, when the PUs resume the spectrum access, which is temporarily occupied by the CUs, then the CUs have to vacate it as soon as possible, without causing any interference. The activity of the PUs can be inferred by using various detection techniques such as matched filtering, energy detection, cyclostationary detection etc. The relevant details can be found in [14]–[17] and in their references. These capabilities make the CR an attractive technique of combating the spectrum scarcity. The spectrum under-utilization motivates the regulatory bodies to officially allow CRs to opportunistically access and exploit the PR spectrum. As a result, the first CR based standard, namely IEEE 802.22 was designed, for wireless regional area networks (WRAN) [18].

In this paper, we propose a Cognitive Go-Back-N HARQ (CGBN-HARQ) scheme operating in a spectrum overlay environment [1], [9], [10], [19], which enables the CU to sense and access the channel licensed to the PUs for its own transmission, given that the channel is free from the PUs at the instant of request [20]–[22]. Similar to the two-state Markov chain of [21], [23], and [24] and to the 'ON'/'OFF' model studied by Saleem and Rehmani [25], in this paper, we model the presence and absence of the PU in the channel by a two-state Markov chain having the 'ON' and 'OFF' states. Specifically, in the 'ON' state, the channel is considered to be occupied by the PUs, whereas in the 'OFF' state, the channel is free and available for the CU's transmission. Furthermore, similar to [20], [26], and [27], we also assume that the PR's channel is partitioned into time-slots (TS) of duration $T$, where each TS is further divided into two segments, namely the sensing time of duration $T_s$ and the data transmission time of duration $T_d = T - T_s$. The sensing epoch is used for detecting the activity of the PUs in the channel, and the remaining time duration is used for data transmission relying on the traditional Go-Back-N HARQ protocol [28]–[30].

The data transmission in the CR environment is similar to the classical techniques used for wireless communication, and hence they also share the same problems imposed by distortion, interference, noise, fading and impairments [31]–[33]. To mitigate these problems and to achieve reliable data transmission, the CR system also require powerful performance-enhancement techniques in both the physical layer (such as error-correction coding, spread spectrum, diversity and equalizer techniques) and in data link layer (such as the frame-length control, error-correction/detection and retransmission), as presented in Fig. 1 [28], [34]. In this regard, both Automatic Repeat ReQuest (ARQ) and Forward Error Correction (FEC) are used for achieving reliable data transmission. In the former, both error-detection and retransmission are employed for reliable data transmission over a noisy channel. In the latter, an error correction code is used. Moreover, for the sake of mitigating the limitations of both techniques and enhancing the overall performance, Hybrid of FEC and ARQ may be employed [28], [35].

To achieve reliable data transmission, our proposed CGBN-HARQ scheme incorporates the traditional GBN HARQ protocol into our CR system. We prefer the GBN HARQ protocol over the stop-and-wait and selective ARQ schemes, because, it has a higher throughput and lower delay than the classic stop-and-wait HARQ (SW-HARQ) and lower complexity than the selective-repeat HARQ (SR-HARQ) [28]–[30]. As mentioned above, when the transmitter deems the channel to be free, it transmits $N$ packets in a chronological order based on GBN-HARQ protocol. On the other hand, the CR receives packets one after the other and generates feedback accordingly for each received packet, which is then conveyed back to the transmitter accordingly. The transmitter always transmits a new packet when an ACK is received whereas, after the reception of a NACK, both the erroneous and the subsequent packets are retransmitted in the next free TSs.

### A. RELATED WORK

CR systems have received considerable research attention [10], [77]–[80]. For example, Sohrabi *et al.* [77] and Buracchini [78] have studied the challenges in hardware, software and implementational issues of SDR. The Federal Communications Commission has issued a number of rules and regulations for allowing the CR systems to exploit the under-utilized spectral bands [3], [4], [81]. Following that, Akan *et al.* [82] as well as Akyildiz *et al.* [83] studied the associated challenges imposed on the OSI protocol stack of CR systems, as shown in Fig. 1. For instance, the physical layer is mainly responsible for channel estimation, for sensing the spectrum and for the reconfiguration of its parameters, such as carrier frequency, the signal detection, modulation, demodulation and encryption of data based on the spectrum decision and the received power [1], [59]. The data link and network layer are mainly responsible for reliable end-to-end data transmission [82], [83]. Bicen and Akan [85] and Bicen *et al.* [86] discussed the challenges in terms of reliability and congestion control as well as delay-sensitive and multimedia data transmission faced by the CR system in various spectrum environment.

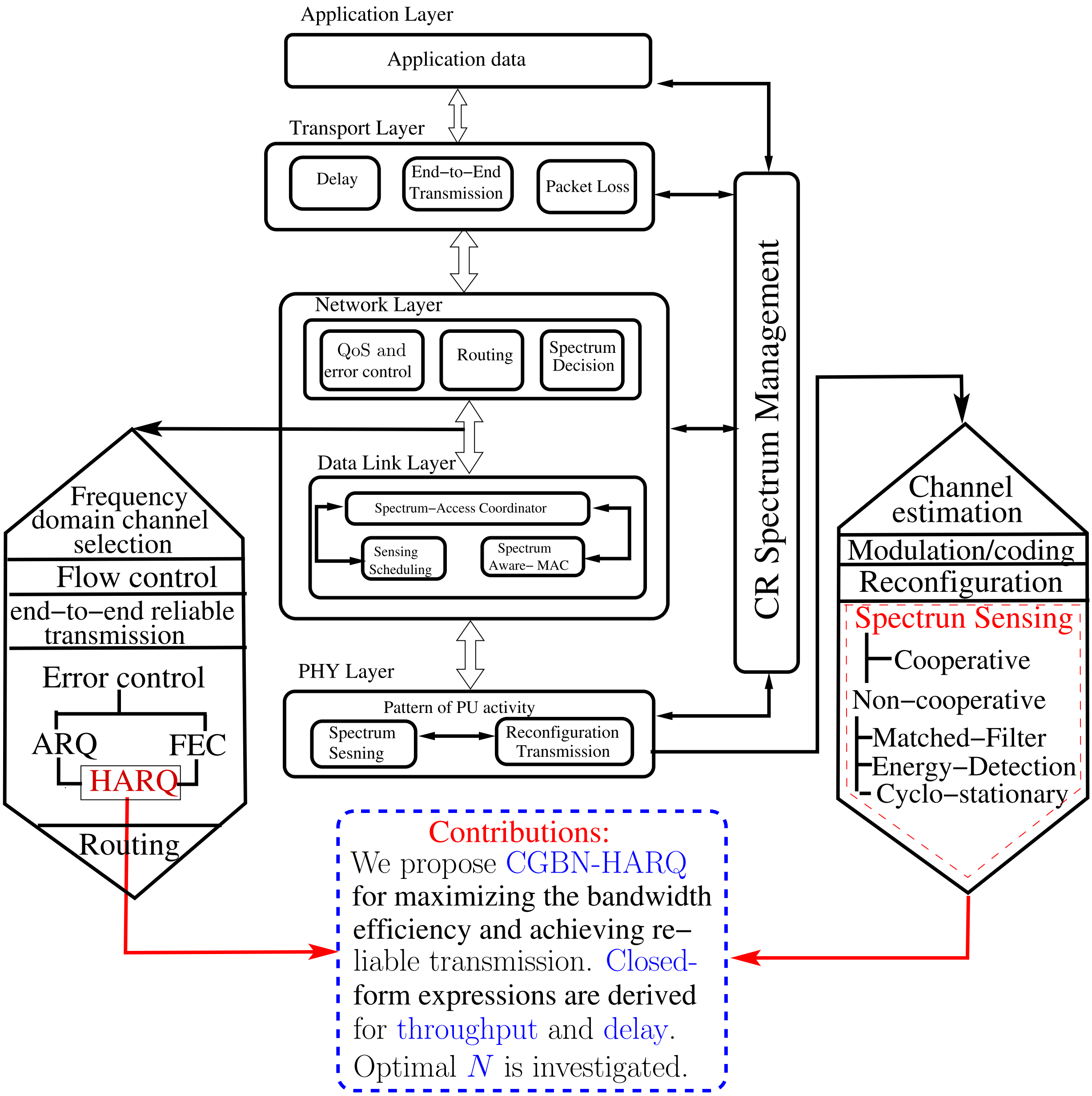


**FIGURE 1.** An overview of the OSI protocol stack in CR systems and novel contributions of this paper.

The throughput of CR networks under the idealized simplifying assumption of perfectly detecting the activity of the PUs has been explored by Yucek and Arslan [16]. The optimal sensing time and the choice of specific sensing techniques have been studied in [15], [20], and [87] whereas the optimal frame-length has been explored in [87]. In a little more detail, Liang *et al.* [20] as well as Tang *et al.* [87] investigated the optimal sensing duration and TS duration for the sake of maximizing the throughput. By contrast, Stotas and Nallanathan [27], focused their attention on the particular sensing techniques as well as transmission protocols, and presented the trade-off between the sensing duration and throughput. Axell *et al.* in [17] studied the state-of-the-art and advancements in CR system which particularly focused on spectrum sensing and detection.

After the successful detection of a free channel, the next task of the CU is to transmit using the transmission protocols. As mentioned above, both the conventional wireless and CR communication systems share the same problem of erroneous transmissions. Hence, powerful error-correction/detection codes have to be used [28], [34]. For instance, in order to attain a high reliability whilst maintaining a high throughput, HARQ has been employed in various communication networks, such as underwater acoustic networks [42], satellite communication [88], in audio as well as video transmissions over the Internet [89] and in multi-relay environments for

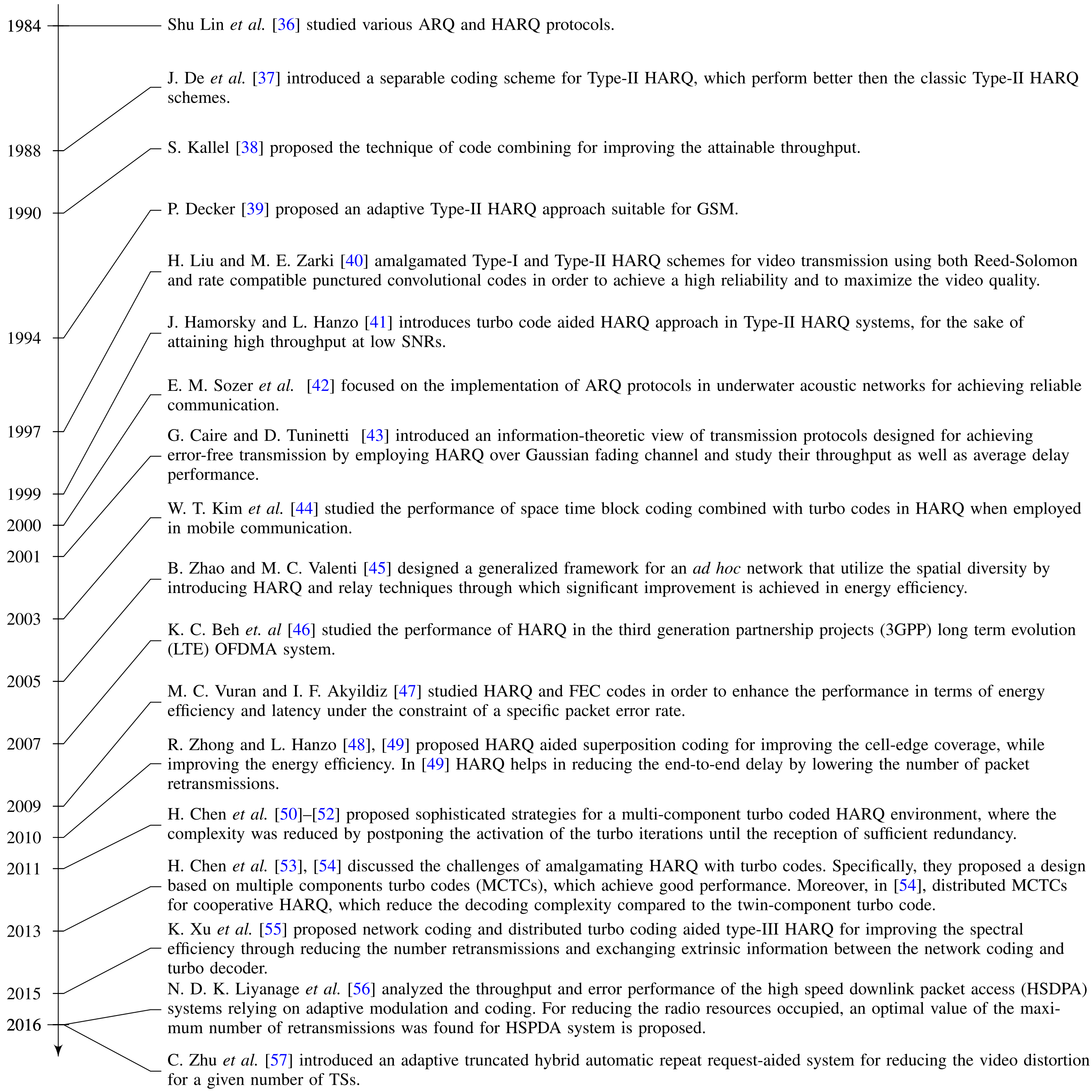


**FIGURE 2.** Timeline of HARQ in wireless communication.

transmission over orthogonal TSs [45]. The HARQ technique has also been invoked in various IEEE standards [90]–[92]. Ngo and Hanzo [93] surveyed the state-of-the-art of the HARQ in the cooperative wireless communication and a novel rely-switching technique is proposed for enhancing the system throughput. Moreover, in Fig. 2, we summarized few major contributions in which HARQ protocols are employed for conceiving reliable transmission.

The operating principle of the classic GBN ARQ protocol has been extensively studied in [28]–[30]. The performance of the conventional Go-Back-N HARQ has been investigated in [94]–[99]. In more detail, Turin [96] and Ausavapattanakun and Nosratinia [99] have modelled the GBN ARQ using hidden Markov chains and investigated the effect of both reliable and unreliable feedback on the throughput. Chakraborty and Liinaharja [97] proposed an adaptive GBN-ARQ protocol in which the transmitter changes its operational mode based on the feedback received. Additionally, Zorzi [98] proposed an error-control scheme in order to improve the performance of the GBN retransmission scheme under the delay constraints. The distribution of packet delay has been studied in [102] and [103].

However, to the best of our knowledge, limited research has been dedicated to analysing and implementing the HARQ protocols in the context of dynamic CR systems. The research carried out in this regard includes [31]–[33], [70], [102]–[110]. However, in these studies, the performance of CR systems employing HARQ protocols has been investigated in terms of the CU throughput, and there is a paucity of exact analytical modelling. For example, the feedbacks concerning the success/failure of the PUs transmission has been used for inferring the presence/absence of the PUs, but without the employment of the ARQ aided protocols [70], [102], [103]. Moreover, Fujii *et al.* [111] introduced space-time-block-coding aided distributed ARQ in an *ad hoc* CR network relying on retransmitting the erroneous packets using ARQ. Additionally, a table is built at the source node based on the interference imposed by the PUs, which helps in finding a sufficiently high-quality channel after each retransmission. This may avoid retransmission. As a further advance, cross-layer operation of the physical layer and MAC layer has been proposed [112]. Jeon and Cho [113] introduced an efficient resource allocation scheme in the context of a multi-hop relaying system, in which the data transmission between the relays takes place using the selective-repeat ARQ protocol. Ahmad *et al.* in [114] explicitly studied the radio resource allocation approaches in context of CR systems. Following that, an end-to-end hybrid ARQ scheme was proposed for end-to-end error control at the session layer [104]. Furthermore, Yue *et al.* [109] as well as Yue and Wang [107] designed improved anti-jamming coding techniques for CR systems to achieve reliable communication.

An adaptive dynamic network coding approach has been proposed in the context of cooperative communication between the PUs and CUs, where bandwidth efficient trellis coded modulation has been used for freeing the PU's bandwidth and for improving the attainable throughput [115]. In order to improve the performance of CUs, spectrum interweave and underlay sharing approaches were consolidated in [112] and [113]. Specifically, Hu *et al.* [110] employed an ARQ technique for enhancing the reliability. Patel *et al.* [116], [117] focused their attention on maximizing the achievable rates of both underlay-based and interweave-based CR systems, when assuming realistic imperfect sensing. Various communication techniques have been surveyed in [31]–[33], [121], and [122]. In Fig. 3, we summarized the evolution of reliable transmission in the context of CR systems.

### B. CONTRIBUTION AND PAPER STRUCTURE

The inspiration of this work is obtained from our previous studies [120]–[122]. We investigated the achievable throughput and delay of Cognitive Stop-and-Wait HARQ (CSW-HARQ) in the light of both perfect and imperfect sensing in [123] and [124]. However, similar to the conventional wireless communication systems, the CSW-HARQ is convenient for implementation, but it is not a high-efficiency ARQ scheme in terms of its throughput and transmission delay. This is because the transmitter in CSW-HARQ scheme transmits a single packet and then waits for its the acknowledgement. During this waiting time the transmitter is not allowed to (re)transmits a packet. On the other hand, a simulation based study is provided in [122], in which the transmitter continuously transmits $N$ packets in a free TS without waiting for their acknowledgement, which are designed to be received after the round-trip-time of $(T_s + T_d)$ seconds. This results in a simplified model for the CR transmitter at the expense of both an increased round-trip delay and retransmissions.

In contrast to [122] and [120], [121], in this treatise, the transmitter assumed to have the ability to continuously transmit $N$ packets and receive feedback flags both during the sensing period as well as in the transmission period of the TS. Since the feedback flags are strongly protected and they require only a single bit of information [123], [124], this overhead does not hamper the sensing process or PU's transmission. These assumptions make the analytical modelling of the proposed scheme more challenging due to the change in the position of packets in the transmitter buffer with respect to 1) the reception of the ACK and NACK flags during the sensing period and 2) the sensing decision. However, it helps the transmitter in avoiding the unnecessary retransmission of packets, whose ACK flags are received during the sensing time, which improves the overall throughput and reduces the delay of the system. Against the above background, in this paper, we extend the solution presented in [122] by deriving new analytical framework, which allows us to derive closed-form expressions both for the throughput as well as for the average packet delay and for the end-to-end packet delay. Our studies show that both the activity of the PR system and the transmission reliability of the CR system imposes a substantial impact on the achievable performance of the CGBN-HARQ. Hence, the parameters may have to be adapted according to the near-instantaneous communication environment in order to maximize its performance.

The main contributions of this paper may be summarised as follows:

(a) A novel cognitive protocol CGBN-HARQ is proposed for CR systems in order to achieve reliable communication. Naturally, the proposed CGBN-HARQ scheme is inspired by the classic GBN-HARQ scheme, but we have to reformulate its transmission regime in order to meet the demanding requirements of CR systems. In our CGBN-HARQ arrangement, the transmitter first has to sense the channel prior to using it. Furthermore, the transmitter may receive feedback information both during the sensing period and the data transmission period.

(b) By modelling this novel CGBN-HARQ arrangement using a discrete time Markov chain, we study both the attainable throughput and the average delay. We derive closed form expressions both for the throughput and the

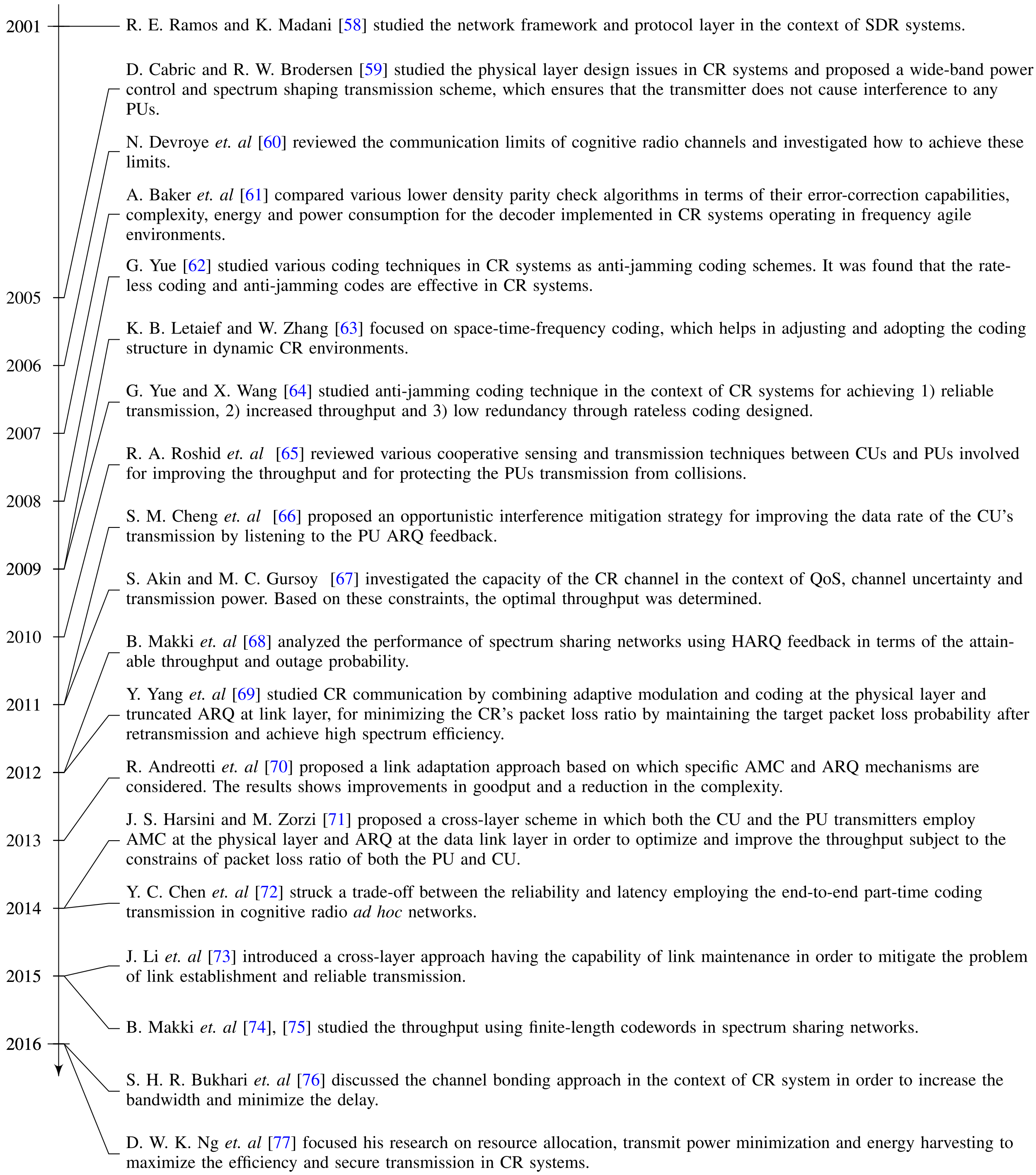


**FIGURE 3.** Timeline of HARQ techniques employed in CR systems.

average delay of the CR systems operated under our CGBN-HARQ scheme.

(c) Equations have been derived for quantifying the end-to-end packet delay performance in terms of its probability distribution and the average end-to-end packet delay.

(d) Finally, a range of simulation results are provided for the verification of our theoretical analysis and for characterizing demonstrate the achievable performance of our CGBN-HARQ scheme.

The structure of this paper is shown in Fig. 4.

## II. SYSTEM MODEL

We continue by formulating both the PR and CR system models used in our analysis.

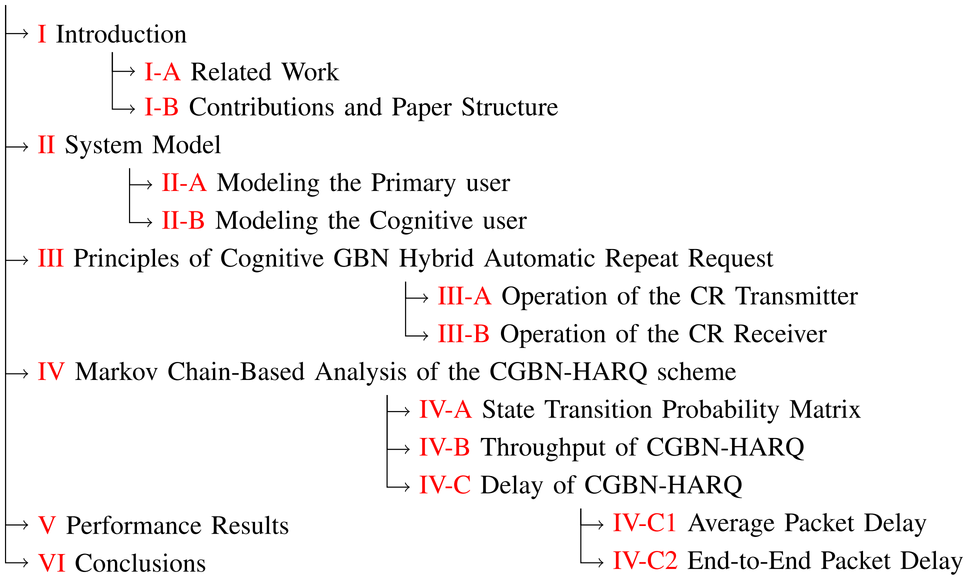


**FIGURE 4.** The structure of this paper.

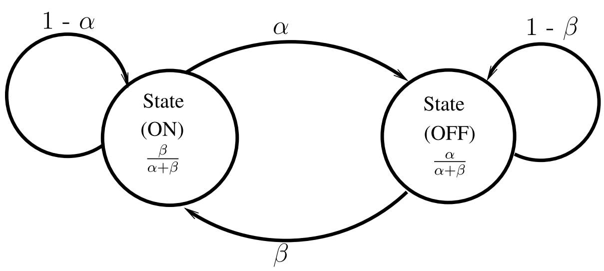


**FIGURE 5.** Discrete-time two-state Markov chain modelling the process of PR system [21], [23], [24].

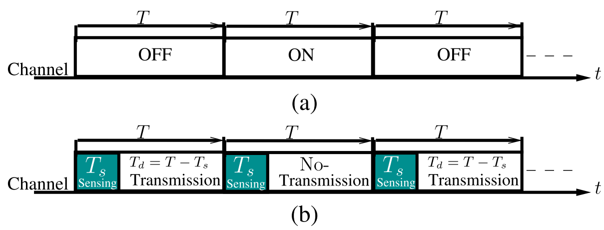


**FIGURE 6.** Time-slot structure of the PR and CR systems, where a CR TS consists of a sensing duration of $T_s$ and a transmission duration of $T_d = T - T_s$ seconds, given the total duration $T$ of a time-slot [20], [26], [27]. (a) Pattern of channel usage by PR. (b) Pattern of channel usage by CR.

### A. MODELING THE PRIMARY USER

As in [120], we consider a PU transmitting in time-slots (TSs) of duration $T$ at an independent and identical probability. This process is modelled as a two-state Markov chain obeying the transition probabilities of Fig. 5, where the 'ON' state represents that the channel is activated by the PUs. By contrast, the state 'OFF' indicates that the channel is free for the CU to use it. In Fig. 5, $\alpha$ and $\beta$ denote the probabilities of traversing from the states 'ON' and OFF' to the opposite states. Let us denote the probabilities of the PU being 'ON' and 'OFF' by $P_{on}$ and $P_{off} = 1 - P_{on}$. Then, in the steady state of Markov model, we have [29]

$$P_{on}\alpha = P_{off}\beta, \tag{1}$$

yielding:

$$P_{on} = \frac{\beta}{\alpha+\beta}, \quad P_{off} = \frac{\alpha}{\alpha+\beta}. \tag{2}$$

Furthermore, as observe in Fig. 6(a) that if PU is in the 'ON' state at the beginning of a TS, it remains active until the end of that TS, hence, it cannot be used by the CU. Naturally, if a TS is not used by the PUs, then it is free for the CU [21], [24], [86]. Note that the state probabilities of the Markov chain determines the 'ON' and 'OFF' durations of the PU.

### B. MODELING THE COGNITIVE USER

The CU obeys the overlay paradigm of [1] and [128], where the CU is only at liberty to use the channel, if it is free from the PUs. We assume perfect activity sensing, yielding no misdetection and no false-alarm. Similar to [20], [26], and [27], each TS is partitioned into the channel sensing duration of $T_s$ and the data transmission duration of $T_d = T - T_s$, as seen in Fig. 6(b). Hence, when the PU is deemed to be in the 'OFF' state within $T_s$, the CU exploits the time duration $T_d$ for its transmission by involving the GBN-HARQ protocol. Additionally, the CU's buffer is always assumed to have data in it.

## III. PRINCIPLES OF COGNITIVE GBN HYBRID AUTOMATIC REPEAT REQUEST

Recall that the CGBN-HARQ regime relies on two main functions, namely channel sensing and data transmission.

Specifically, at the commencement of a TS, channel sensing is used for ascertaining whether the TS is busy or free. Provided that the TS is deemed to be free, transmission ensures using a Reed-Solomon (RS) code RS($N_d$, $K_d$) [28] defined over the Galois-field GF(q), where $K_d$ and $N_d$ denote the number of original information symbols and coded symbols,respectively. Each RS codeword encodes a packet, which is transmitted within $T_p$ seconds. Upon arranging for $N = T_d/T_p$, the CR transmitter conveys $N$ packets per TS. The RS code is capable of correcting number of $t = (N_d - K_d/z)$ symbol errors and that reliable cyclic redundancy check (CRC) codes are used for detecting, if there are uncorrectable errors in a received packet.

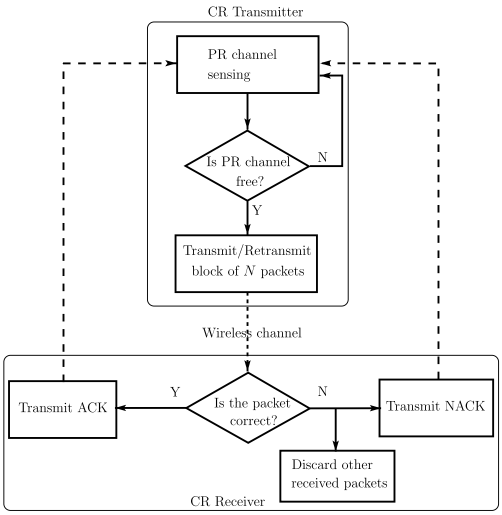


**FIGURE 7.** Flow chart showing the operations of the proposed CGBN-HARQ scheme.

This CGBN-HARQ protocol sequentially transmits $N$ packets, while waiting for the corresponding feedback. Explicitly, $N$ represents the maximum number of packets transmitted during the round-trip time (RTT), which is assumed to be $T_d$. Note that the RTT is defined as the time interval between the transmission of a packet and the reception of a feedback for the same packet. The operation of the CGBN-HARQ protocol of Fig. 7 is described by Algorithm 1 which is mainly organized in two steps.

- In the first step, the transmitter transmits packets in the sensed free TS. Following that, if the ACK flags are received after the elaps of the sensing time, then the transmitter keeps on transmitting new packets until the end of the TS (i.e., $(N-k)$ seconds), as stated on Line 16. On the other hand, if the ACK flags are received within the sensing time or in a busy TS, then the transmitter remains silent, as stated on Line 21. Moreover, if a NACK flag is received, the algorithm returns to Line 6 and provided that the TS is free, the $i$th erroneous and $(N - c + i - 1)$ subsequent packets are retransmitted, where $c$ is the counter keeping track of packets that have already been transmitted in the current TS.
- Secondly, the receiver generates feedback flags based on the error-free or erroneous reception of packet, as stated on lines 11 and 25, respectively, and sends them to the transmitter accordingly.

### A. OPERATIONS OF THE CR TRANSMITTER

The transmitter of conventional GBN-HARQ, continuously transmits packets, until a NACK signal is received. In presence of decoding errors both the error-infested packet as well as the other packets transmitted after the corrupted packet are retransmitted. By contrast, observing both Algorithm 1 and Fig. 7, in our proposed CGBN-HARQ scheme, the CU is only allowed to transmit packets in the TSs free from the PUs. Hence, the CU has to sense PU's presence/absence before the transmission or retransmission of packets. If the PU is in its 'OFF' state, the CR transmitter transmits $N$ packets, which may include both new packets and the corrupted packets requiring retransmission. Otherwise, the transmitter waits for the next TS and senses the channel again. In our scheme, we assume that all packets are of the same length and the CR transmitter is always ready to transmit these packets in free TSs. Furthermore, each CU packet consists of a RS coded codeword, which is transmitted within the duration of $T_p$ seconds, as shown in Fig. 8. The feedback of each packet is received after the RTT of $T_d = NT_p$ seconds, where again $T_s = 1T_p$ is assumed.

It is worth mentioning that for implementing the CGBN-HARQ, the CR transmitter is assumed to have a buffer of size $N$, which follows the FIFO principle [28]–[30]. The transmitter stores the transmitted packets in its buffer until they are positively acknowledged (ACK). The buffer is updated according to the feedbacks gleaned from the CR receiver. Therefore, if the CR transmitter receives a positive ACK for a packet, its copy is deleted from the buffer and a new packet is appended at the end. Otherwise, no new packet is appended and both the erroneous packet as well as the subsequent packets are retransmitted in the next free TS.

We also assume that the CR transmitter is capable of receiving feedback for the transmitted packets both during the sensing period and the data transmission period, regardless of whether the channel is free or not. The ACK/NACK feedback signals are assumed to be always error-free, which is justified by the fact that the feedback signals are usually well protected [123], [124]. Moreover, the information content is usually low, since a single bit is enough for the CGBN-HARQ. Therefore, the reception of feedback can be readily protected from errors and it does not adversely affect the sensing and transmission processes.

Owing to the above assumptions, the CGBN-HARQ protocol has two scenarios for the reception of feedback: 1) reception of feedback within the sensing periods; and 2) reception of feedback outside the sensing periods, as shown in Figs. 8, 9 and 10.

In the first case, when a feedback is received within a sensing period, as stated on line 21 of Algorithm 1, if the ACK of a transmitted packet is received, then the CR transmitter

**Algorithm 1** CGBN-HARQ Algorithm

1: **Initialization**: $M_c$ = number of packets, $T_d = NT_p$, $T_s = kT_p$, $i = 1$, $c = 0$, $P_t = 0$, TS= 1.
2: **Input:** $N$, $k$, packets.
3: **while** $i \leq M_c$ **do**
4:     CR transmitter senses a TS.
5:     **if** TS is free **then**
6:         Transmit packets from $i$ to $N - c + i - 1$.
7:         TS = TS +1, $j = i$.
8:         Transmitter starts sensing next TS immediately.
9:         **while** $j \leq N - c + i - 1$ **do** ▷ Check each received packet.
10:             **if** the $j$th packet is received error-free **then**
11:                 receiver transmits ACK for the $j$th packet.
12:                 $j = j + 1$.
13:                 **if** TS is free && ACK is received in $T_d$ period **then**
14:                     Transmit a new packet i.e. $P_t = (N - k) + (j - 1)$.
15:                     $c = c + 1$; ▷ Counter of packets transmitted
16:                     **if** $c == N - k$ **then**
17:                         Transmit packets from $(P_t + 1)$ to $N + j - 1$.
18:                         **Set** $c = 0$, TS = TS +1, $i = j$ and **Goto** line 8.
19:                     **end if**
20:                 **else**
21:                     TS is busy || ACK is received in $T_s$
22:                     No transmission and wait.
23:                 **end if**
24:             **else**
25:                 reciever transmits NACK for the $j$th packet and discard the following packets.
26:                 **if** TS is free || NACK is received during $T_s$ or $T_d$ **then**
27:                     **Set** $i = j$, **Goto** Line 6
28:                 **else**
29:                     TS is busy && NACK is received.
30:                     No transmission and wait.
31:                     **Set** $c \leftarrow 0$, $i = j$ and **Break**.
32:                 **end if**
33:             **end if**
34:         **end while**
35:     **else**
36:         Waits until the next TS.
37:     **end if**
38:     TS=TS+1.
39: **end while**

deletes the copy of the corresponding packet from its buffer and continues to transmit new packets in the next free TS, as shown in Fig. 8. On the other hand, when a NACK of a transmitted packet is received during a sensing period, then the CR transmitter prepares to retransmit the erroneous packet as well as its $(N - 1)$ subsequent packets in the next free TS, as depicted in Fig. 9.

In the context of the second case, as shown in Fig. 10, a feedback is received for a transmitted packet in the next TS, after a sensing period, which is presented on line 13 of Algorithm 1. If the next TS is sensed to be free and an ACK signal is received, a new packet waiting in the buffer is then transmitted immediately. By contrast, if a NACK signal is received, the corresponding erroneous packet as well as its subsequent discarded packets have to be retransmitted, and the erroneous packet is retransmitted immediately. However, if a NACK signal is received during a busy TS, then the erroneous packet and its $(N - 1)$ subsequent packets are transmitted during the next free TS, as shown in Fig. 10.

### B. OPERATIONS OF THE CR RECEIVER

The CR receiver operates similarly to the conventional GBN-HARQ. In the CGBN-HARQ, the CR receiver is assumed to have a buffer for storing the index of the received packets [29], [30], which increases by one only when an error-free packet is received, as presented in Algorithm 1. In detail, the

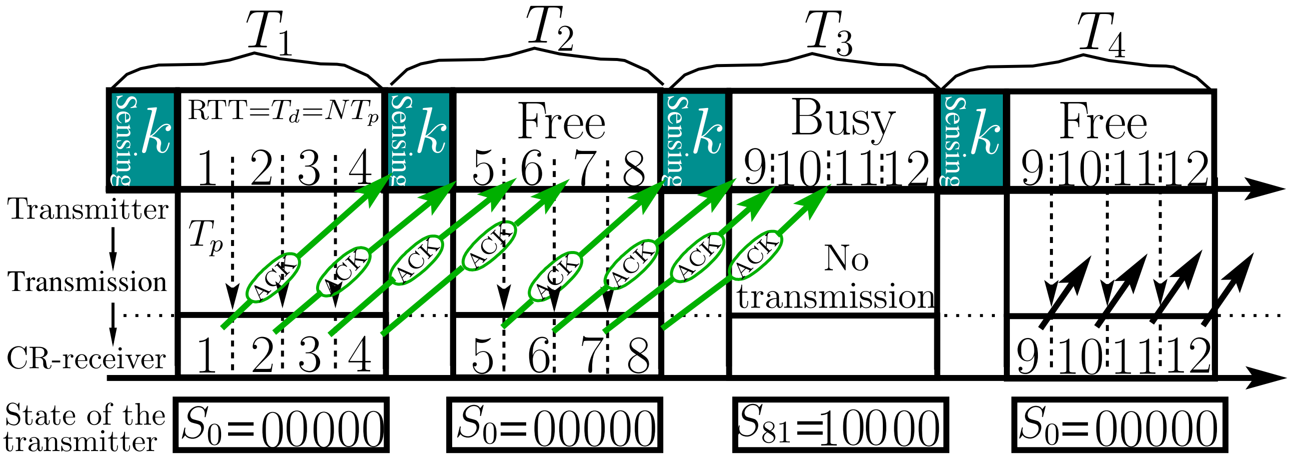


**FIGURE 8.** Transmission flow of the CGBN-HARQ scheme with the parameters of $k = 1$ and $N = 4$, when assuming the ideal scenario that all packets are correctly received.

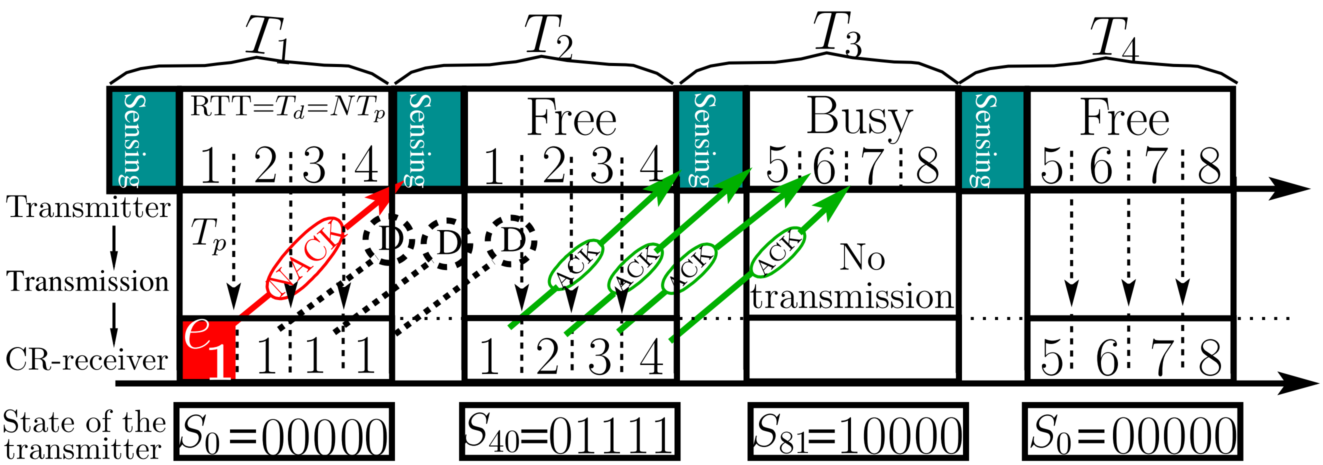


**FIGURE 9.** The transmission flow of CGBN-HARQ using $k = 1$ and $N = 4$ when an erroneous packet is received during a sensing period. The *green* and *red* solid lines represent error-free and erroneous transmission, whereas the dotted lines depict the discarded packets. The box with letter '*e*' shows the position of the erroneous packet in the TS.

operations of the CR receiver can be explained in terms of its *normal state* and *erroneous state*, as follows.

### 1) NORMAL STATE

The CR receiver is considered to be operated in the normal state, when the index of a received packet matches the sequence number stored in the receiver buffer. If this is the case, the CR receiver first carries out RS decoding, then it generates the corresponding ACK or NACK signal, to be sent to the CR transmitter. Furthermore, if the packet becomes error-free after RS decoding, the CR receiver increases the index by one, as stated on lines 11 and 12 of Algorithm 1. Then, the CR receiver waits for the reception of the next packet.

### 2) ERRONEOUS STATE

When the CR receiver is in the normal state but an erroneous packet is received after RS decoding, the CR receiver changes to the erroneous state. During this state, the receiver discards the erroneous packet and transmits a NACK flag to the CR transmitter. Furthermore, the index in the CR receiver buffer remains unchanged. Additionally, the CR receiver discards the subsequent packets received within the period $(N-1)T_p$ following the erroneous packet, regardless of whether they are correct or not, as stated on line 25 of Algorithm 1. Following the above actions, the CR receiver enters into the normal state and waits for receiving the retransmission of the erroneous packet.

As the example of Fig. 10 shows, when the CR receiver finds that *packet* 3 is in error, it discards the erroneous *packet* 3 as well as the pair of subsequent packets, i.e. *packets* 4 and 5, since the CR receiver has to first correctly receive *packet* 3. Furthermore, as shown in Fig. 10, after the reception of a NACK for *packet* 3, the CR transmitter stops transmitting new packets and immediately retransmits *packet* 3 as well as the other packets already transmitted, provided that there

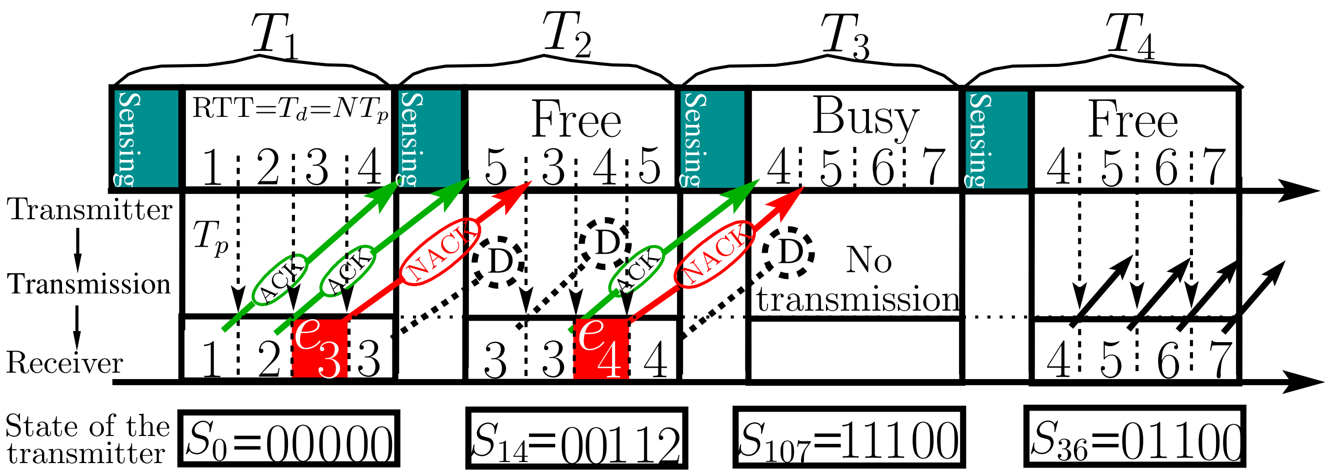


**FIGURE 10.** Transmission flow of CGBN-HARQ scheme using $k = 1$ and $N = 4$, when a NACK is received after a sensing period followed by a free TS and a NACK is received within a busy TS.

are free TSs for transmission. The above process continues until all packets have been successfully received by the CR receiver.

## IV. MARKOV CHAIN-BASED ANALYSIS OF THE CGBN-HARQ SCHEME

Similar to the classic GBN-HARQ, the operations of our CGBN-HARQ can also be modelled with the aid of a discrete-time Markov chain (DTMC). However, as the CR system can only access the PU channel, when the channel is set free by the PUs, the modelling and analysis of the CGBN-HARQ become challenging. In this section, we propose a technique of circumventing the challenges of modelling the CGBN-HARQ as an DTMC. Based on our modelling technique, both the attainable throughput and the delay performance of the CGBN-HARQ will be analyzed in Sections IV-B and IV-C.

We assume that states are defined with respect to the TSs, i.e. the state transition rate is synchronized with the TSs. The state of a TS is jointly determined by the 'ON' or 'OFF' state of the PU and the 'new packet', 'retransmitted packet', and 'packet repeated in one TS' states of the contents stored in the CR transmitter's buffer, when the buffer is observed at the end of a TS. In more detail, let us express the list of states as

$$\mathbb{S} = \{S_0, S_1, \ldots, S_i, \ldots\}. \tag{3}$$

The total number of states is denoted by $S_T$, where we have $S_T = |\mathbb{S}|$, and $S_i$ is the $i$th legitimate state, which is a $(N+1)$-length base-3 digit expressed as

$$S_i = S_{i0}S_{i1}\cdots S_{iN}, \quad i = 0, 1, \cdots \tag{4}$$

where $S_i$ is also referred to as the $i$th state sequence. In (4), the definition of $S_{i0}$ is

$$S_{i0} = \begin{cases} 0, & \text{if the considered TS is free} \\ 1, & \text{if the considered TS is busy,} \end{cases} \tag{5}$$

while the definition of $S_{ij}$, $j = 1, \ldots, N$, is

$$S_{ij} = \begin{cases} 0, & \text{if the } j\text{th packet is a new one;} \\ 1, & \text{if the } j\text{th packet is a retransmitted one when the TS is free, or one to be retransmitted when the TS is busy;} \\ 2, & \text{if the } j\text{th packet is a repeated one of a previous packet in the same TS.} \end{cases} \tag{6}$$

Based on the definitions of (5) and (6), we can find a one-to-one mapping for $i$ of $S_i$ as

$$i = \sum_{j=0}^{N} S_{ij}3^{N-j} \tag{7}$$

Below we use a pair of examples to briefly introduce the principles of modelling and the state transitions. First, let us consider a simple CGBN-HARQ scheme, which has the parameters of $k = 1$ and $N = 1$, implying that the CR transmitter uses a single $T_p$ interval for channel sensing and the transmitter buffer stores a single packet transmitted/retransmitted or to be transmitted/retransmitted in a TS. In this case, we should note that the third case in (6) will never occur, implying that no packet will be repeated within a specific TS and the digit 2 of (6) will never appear. Then, according to the above definitions, the corresponding DTMC has 4 states, which are $S_0 = 00$, $S_1 = 01$, $S_3 = 10$ and $S_4 = 11$. The state $S_2 = 02$ never appears.

The state diagram associated with the transitions is shown in Fig. 11. In this simple CGBN-HARQ scheme, the transition probabilities can be readily found. For example, assuming that the CGBN-HARQ is currently in state $S_0 = 00$, which means that the current TS is free and a new packet transmitted, when the packet is correctly received by the CR receiver and the next TS is also sensed to be free, the next state will also be $S_0 = 00$. Correspondingly, the transition

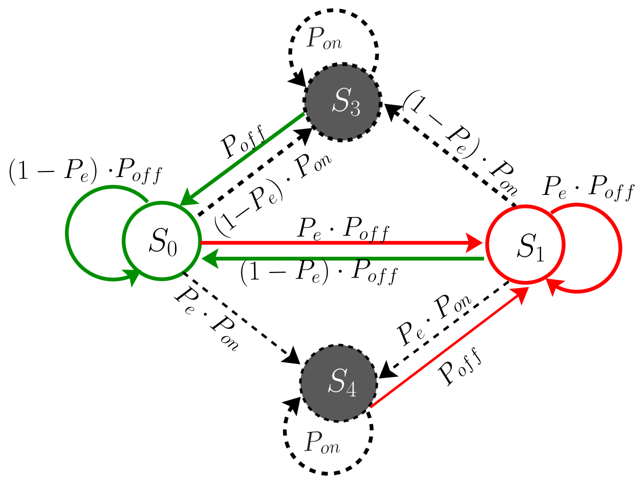


**FIGURE 11.** State diagram of the CGBN-HARQ scheme with $N = 1$ and $k = 1$, *dashed* lines correspond to the transitions towards the busy states $S_3 = 10$ and $S_4 = 11$, *solid* lines illustrate the transitions towards free state $S_0 = 00$ and $S_1 = 01$, while *red* and *green* lines correspond to that the packet is received error free and received in error, respectively.

probability is $P_{0,0} = P_{off}(1 - P_e)$, as shown in the Fig. 11, where $P_{off}$ is the probability that the TS is free and $P_e$ is the error probability of receiving a corrupted packet. By contrast, when the packet is received in error and the next TS is free, the next state will be $S_1 = 01$. Correspondingly, the state-transition probability is $P_{0,1} = P_{off}P_e$. Furthermore, when the packet is received error-free and the next TS is sensed to be busy, the next state will become $S_3 = 10$ associated with a transition probability of $P_{0,2} = P_{on}(1 - P_e)$, where $P_{on} = 1 - P_{off}$, as shown in Section II-A. Similarly, we can analyze the other state-transitions and transition probabilities, which are all shown in Fig. 11.

In the second example, we assume the parameters of $k = 1$ and $N = 4$. Then, let us return to Fig. 10 for considering the special cases that are not shown in the Fig 11. As shown in Fig. 10, the first TS is free and 4 new packets are transmitted. Hence, the state of the CGBN-HARQ is $S_0 = 00000$. The second TS is also sensed to be free. However, the third packet sent in the first TS is received in error. In this case, as shown in Fig. 10, the packets transmitted in the second TS are packets 5, 3, 4 and 5. Correspondingly, the state is $S_{14} = 00112$, and the probability of transition from $S_0$ to $S_{14}$ is $P_{0,14} = P_{off}(1 - P_e)^2P_e$. Following the second TS, the third TS is found to be busy. Furthermore, among the packets transmitted in the second TS, packet 3 is successfully delivered, while packet 4 is received in error. Hence, during the third TS, the packets stored in the transmitter buffer and to be transmitted in the next free TS are packets 4, 5, 6 and 7. Correspondingly, the state is $S_{107} = 11100$, and the state-transition probability from $S_{14}$ to $S_{107}$ is $P_{14,107} = P_{on}(1 - P_e)P_e$. Then, as shown in Fig. 10, the fourth TS is free to use and packets 4, 5, 6 and 7 are transmitted, which yields a state of $S_{36} = 01100$ associated with a transition probability of $P_{107,36} = P_{off}$ from $S_{107}$. Similarly, we can analyze the transitions in the other cases, as and when the various situations are considered.

According to the principles of the CGBN-HARQ and to the above examples, we may infer that the DMTC exhibits the following characteristics.

- When a TS is in 'ON' state, i.e. when we have $S_{i0} = 1$, digit 2 does not appear in the corresponding state sequence.
- When a transition changes from an 'ON' state to an 'OFF' state, $S_{i0} = 1$ in the current state sequence is changed to $S_{i0} = 0$ in the new state sequence, while all the other digits in the state sequence retain the same. Hence, owing to the above observations, the new state sequence does not contain the digit 2 of (6).
- The first digit, i.e., $S_{i1}$, never takes the value of 2 seen in (6).

Although we can remove a lot of states from consideration based on the above-mentioned characteristics, it still remains extremely hard to mathematically derive a formula for calculating the total number of states as well as to represent the state sequences in some general expressions. However, once we know the states and their relationship, we can readily determine the corresponding transition probabilities. In this paper, we propose the Algorithm, of Fig. 12 for finding the states or state sequences. The algorithm is detailed as follows.

In our algorithm, we assume that the CR transmitter starts transmitting $N$ new packets using a free TS, which gives a state $S_0 = 0, 0, \ldots, 0$ of $(N + 1)$ zeros. Therefore, the set of states $\mathbb{S}$ initially contains $S_0$. In order to generate new states from the current state of $S_{cur} = S_0$, we allow errors occur at all the possible positions of the state $S_{cur}$, and also consider both free and busy TSs. For example, as shown in Fig. 9, if the first packet is received in error and the next TS is found to be free, then the transmitter retransmits both the erroneous packet and the discarded packets. Our algorithm assists in generating a new state $S_{40} = 01111$, where the first digit 0 indicates that the TS is free, while the remaining digits represent that four old packets are retransmitted. After the generation of a new state, for example $S_{40}$, it is then compared to all the existing states in $\mathbb{S}$. If it is not contained in $\mathbb{S}$, the state is then concatenated to the end of $\mathbb{S}$. Otherwise, it is deleted.

After generating all the possible new states from state $S_0$, the algorithm moves to the next state $S_l$ in $\mathbb{S}$, which is $S_{40}$ for the example of Fig. 9. The state $S_l$ is then set as the current state and the above procedure is repeated in order to derive other possible states. Since the Markov chain is irreducible and aperiodic, the algorithm is finally terminated, when all the states in $\mathbb{S}$ have been considered as the current states, but without generating new states. At the end of the algorithm, the cardinality of set $\mathbb{S}$ is given by the total number of states $S_T$, i.e., $S_T = |\mathbb{S}|$.

### A. STATE TRANSITION PROBABILITY MATRIX

The probability of transition from one state to another is recorded in the state-transition probability matrix $\mathbf{P}$. Let the state of the $i$th TS be represented by $S(i)$. Then, in the example shown in Fig. 9 and discussed in Section III-A, we have

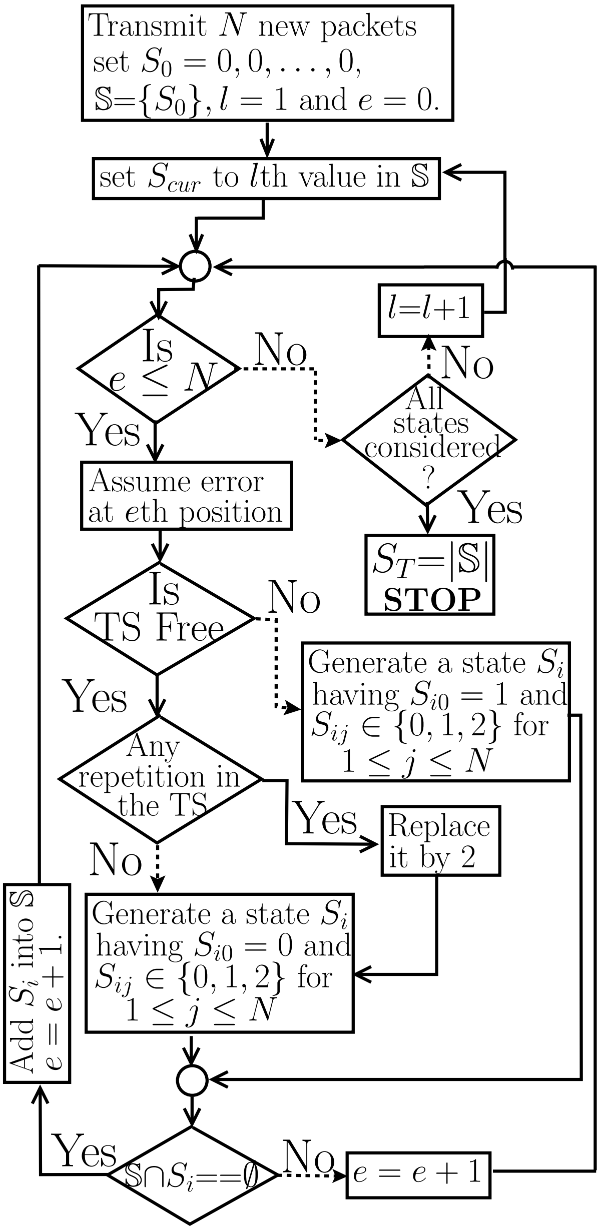


**FIGURE 12.** The flow chart illustrates the process of generating states represented by $(N + 1)$-length base-3 digits. In each state, the TS is either free (0) or busy (1) as well as it has new (0) and/or old (1) and/or repeated (2) packets. $e$ represents the position of the erroneous packet in the TS, while $e = 0$ is a special case when all the received packets are error-free.

$S(1) = S_0$, $S(2) = S_{40}$, $S(3) = S_{81}$ and $S(4) = S_0$. Given the state $S_i$ during TS $t$, the probability $P_{i,j}$ that the next state is $S_j$ during the $(t + 1)$st TS is [29], [126].

$$\begin{aligned} P_{i,j} &= P\left\{S(t+1) = S_j \mid S(t) = S_i, \ldots S(1) = S_0\right\} \\ &= P\{S(t+1) = S_j | S(t) = S_i\}, \quad \text{where } S_i, S_j \in \mathbb{S}. \end{aligned} \tag{8}$$

According to the properties of the DTMC, we have

$$\begin{aligned} 0 \leq P_{i,j} \leq 1 \\ \sum_{S_j \in \mathbb{S}} P_{i,j} = 1, \quad \forall S_i \in \mathbb{S}. \end{aligned} \tag{9}$$

As an example, let us consider the simple example of $N = 1$ and $k = 1$, having the state-transitions shown in Fig. 11. We have demonstrated in Section IV that the DTMC has the state space of

$$\mathbb{S} = \{S_0, S_1, S_3, S_4\}. \tag{10}$$

We can now readily show that the state-transition matrix is

$$\mathbf{P} = \begin{bmatrix} P_{0,0} & P_{0,1} & P_{0,3} & P_{0,4} \\ P_{1,0} & P_{1,1} & P_{1,3} & P_{1,4} \\ P_{3,0} & P_{3,1} & P_{3,3} & P_{3,4} \\ P_{4,0} & P_{4,1} & P_{4,3} & P_{4,4} \end{bmatrix} = \begin{bmatrix} (1-P_e)P_{off} & P_eP_{off} & (1-P_e)P_{on} & P_eP_{on} \\ (1-P_e)P_{off} & P_eP_{off} & (1-P_e)P_{on} & P_eP_{on} \\ P_{off} & 0 & P_{on} & 0 \\ 0 & P_{off} & 0 & P_{on} \end{bmatrix}.$$

Let the probability that the transmitter is in state $S_i$ during TS $n$ be expressed as $P_i(n)$. Then, we have $\sum_{i \in \mathbb{S}} P_i(n) = 1$. Let $\boldsymbol{p}(n) = [P_0(n), P_1(n), \ldots, P_{S_T}(n)]^T$ collect all the $S_T$ probabilities in TS $n$. Furthermore, let us assume that the transmitter starts transmitting, when it is in state $S(1) = S_0$, meaning that

$$\boldsymbol{p}(1) = [1, 0, \ldots, 0]^T. \tag{11}$$

Then, by the law of total probability [29], [127], the probability that the DTMC traverses to state $j$ at TS $(n + 1)$ can be written as

$$P_j(n+1) = \sum_{\forall S_i \in \mathbb{S}} P_i(n) P_{i,j} \quad \forall S_j \in \mathbb{S} \text{ and } n \geq 1. \tag{12}$$

Upon considering all the $S_T$ possible states in $\mathbb{S}$, we have arrive at recursive equation of

$$\boldsymbol{p}(n+1) = \mathbf{P}^T \boldsymbol{p}(n), \quad n = 1, 2, \ldots \tag{13}$$

From this equation, we can readily infer that

$$\boldsymbol{p}(n+1) = (\mathbf{P}^T)^n \boldsymbol{p}(1). \tag{14}$$

As shown in Equation (9), the sum of each column of $\mathbf{P}^T$ is 1. Hence, the transition matrix $\mathbf{P}^T$ is a left stochastic matrix. Then, according to the *Perron-Frobenius theorem*, the limit of $\lim_{n\to\infty}(\mathbf{P}^T)^n$ exists [127]. Consequently, when $n \to \infty$, the Markov chain reaches its steady state [29] and hence we have

$$\boldsymbol{p}(n+1) = \boldsymbol{p}(n). \tag{15}$$

Let the steady-state probabilities be expressed by $\boldsymbol{\pi}$, i.e. we have $\boldsymbol{\pi} = \lim_{n\to\infty} \boldsymbol{p}(n)$. Then, from (15) we have [29], [126],

$$\boldsymbol{\pi} = \mathbf{P}^T \boldsymbol{\pi}, \tag{16}$$

which shows that the steady state probability vector $\boldsymbol{\pi}$ is the right eigenvector of $\mathbf{P}^T$, corresponding to the eigenvalue of one. Therefore, $\boldsymbol{\pi}$ can be obtained via calculating the eigenvector of $\mathbf{P}^T$ [29], [126], [127]. Note that the steady state probabilities satisfy the following constraint of

$$\sum_{S_j \in \mathbb{S}} \pi_j = 1 \quad \text{or } \boldsymbol{\pi}^T \times \mathbf{1} = 1, \tag{17}$$

where $\mathbf{1}$ represents an all-one column vector.

### B. THROUGHPUT OF CGBN-HARQ

The throughput of the CGBN-HARQ is defined as the average number of successfully transmitted packets per TS [28], [128]. As mentioned previously, in CGBN-HARQ, successful transmission of a packet in a TS is achieved, when 1) the TS is free; and 2) error-free transmission of the packet using the free TS is achieved. Given the steady-state probabilities of (16) and the state transitions, the throughput ($R_s$) of the CGBN-HARQ can be analyzed as follows.

When the DTMC reaches its steady-state, its throughput is only dependent on the following two events a) The PU channel is free, implying that the first digit of the state sequence is zero. Hence, considering that the length of state sequences is $(N+1)$ and the digits are base-3 digits, the states contributing to the throughput should have an index lower than $3^N$; b) the number of new packets transmitted with in the state, when then PU channel is free.

Let $n_p(S_i)$ be the number of new packets associated with the state $S_i$ with $i < 3^N$, which equals to the number of zeros in the state sequence of $S_i$ minus one, since the first zero is only an indicator that the PU channel is free. Then, given the steady state probabilities $\boldsymbol{\pi}$, the throughput of the CGBN-HARQ scheme can be expressed as

$$R_s = \sum_{S_i \in \mathbb{S}, i<3^N} \pi_i \times n_p(S_i), \text{ (packets / TS)}. \quad (18)$$

Furthermore, if we express the attainable throughput in terms of the number of packets per $T_p$ (packet duration), we have,

$$R'_s = \frac{T_p}{T} \times R_s = \frac{1}{k+N} \times R_s \quad \text{(packets / } T_p\text{)}. \quad (19)$$

Let us now continue by analyzing the delay performance of the CGBN-HARQ.

### C. DELAY OF CGBN-HARQ

In the classic GBN-HARQ, the packet delay includes both the duration of the first transmission as well as that of any retransmission of the packets. By contrast, in our CGBN-HARQ, the packet delay includes not only that of the traditional GBN-HARQ, but also the duration of waiting for free channels. Hence, in the traditional GBN-HARQ, the delay performance can be simply characterized by the average packet-delay. By contrast, in our CGBN-HARQ, there are two types of delays, both of which provide unique insights into the performance of the CGBN-HARQ systems. The first type is the average packet-delay while the second one is the end-to-end packet-delay. Here, the average packet-delay is given by the total time spent by a CR transmitter between the start of sensing a TS until the successful delivery of all packets, divided by the number of packets transmitted. By contrast, the average end-to-end delay is the average duration from the start of transmitting of a packet until it is confirmed to be successfully received. Below we consider both of these delays.

#### 1) AVERAGE PACKET DELAY ($T_D$)

The average packet delay $T_D$ can be quantified in terms of the average number of TSs (or $T_p$'s) required for the successful transmission of a packet. Hence, given the throughput formulated in (18) or (19), we can readily express the average packet-delay as

$$T_D = \frac{N_t}{N_s} = \frac{1}{R_s} \quad \text{(TS per packet)} \quad (20)$$
$$= \frac{k+N}{R_s} \quad (T_p \text{ per packet}). \quad (21)$$

#### 2) END-TO-END PACKET DELAY

In this subsection, we investigate the end-to-end packet-delay. First, we study the probability distribution of the end-to-end packet-delay. Then, the average end-to-end packet-delay of CGBN-HARQ is evaluated.

Let $\mathbb{S}_N \subset \mathbb{S}$ be a subset of $\mathbb{S}$, which contains all the states associated with new packets transmitted. Given $S_i \in \mathbb{S}_N$, we define a set $\mathbb{S}_i^{(m)}$, which contains all the states $S_j$ emerging from state $S_i$ to state $S_j$, in which there are $l_{i,j} \geq 1$ correctly received new packets with exactly $mT_p$ of delay, i.e. we have

$$\mathbb{S}_i^{(m)} = \{S_j | \text{emerging from } S_i \text{ to } S_j, \text{ there are } l_{i,j} \geq 1 \text{ new packets transmitted in state } S_i \text{ that are correctly received in state } S_j \text{ with the exactly } mT_p \text{ of delay}\}. \quad (22)$$

Furthermore, let the number of new packets transmitted while in state $S_i$ be expressed as $L_i$. Then, the probability mass function (PMF) of the end-to-end packet-delay can be expressed as:

$$P(m) = \frac{1}{c} \sum_{S_i \in \mathbb{S}_N} \sum_{S_j \in \mathbb{S}_i^{(m)}} \frac{\pi_i \times l_{i,j} \times P_{i,j}^{(m)}}{L_i}, \quad \text{for } m = 1, 2, \ldots. \quad (23)$$

where we have $c = \sum_{S_i \in \mathbb{S}_N} \pi_i$ and $P_{i,j}^{(m)}$ denotes the probability of traversing from state $S_i$ to state $S_j$ after the delay of $mT_p$.

Now, given $\boldsymbol{\pi}$, $\mathbf{P}$ and $\mathbb{S}$, the PMF of end-to-end packet-delay can be derived as follows. Let us define:

$$\mathbf{P}_{MF} = [P(1), P(2), \ldots, P(M_T)]^T, \quad (24)$$

where $M_T$ is the highest delay considered, which can be set to a high value so that the probability of having such a delay becomes very small, such as $10^{-8}$. We first initialize $\boldsymbol{p}$ to a vector whose element corresponding to $S_i \in \mathbb{S}_N$ equals one, while all the other elements are equal to zero. In other words, $\boldsymbol{p} = \boldsymbol{I}_i$ represents a single column of the identity matrix $\boldsymbol{I}_{S_T}$. Then, according to the fundamental properties of DTMC, the state-transitions are described by the following recursive equation

$$\boldsymbol{p}^{(j)} = \mathbf{P}^T.\boldsymbol{p}^{(j-1)} = \cdots = (\mathbf{P}^T)^j \boldsymbol{I}_i, \quad j = 1, 2, \ldots \quad (25)$$

From (25) we can see that whenever we multiply $\mathbf{P}^T$ on the current $\boldsymbol{p}^i$, we obtain the following information:

(a) For $P_{on} = 0$

| $P_e$ | $N$ | $R_s$ | $T_D$ | $\tau$ |
|---|---|---|---|---|
| 0 | 1 | 0.5 | 2 | 1 |
| | 2 | 0.66 | 1.5 | 1 |
| | 3 | 0.75 | 1.33 | 1 |
| | 4 | 0.8 | 1.25 | 1 |
| | 5 | 0.83 | 1.2 | 1 |
| | 6 | 0.86 | 1.16 | 1 |
| | 7 | 0.87 | 1.14 | 1 |
| 0.2 | 1 | 0.4 | 2.5 | 1.5 |
| | 2 | 0.48 | 2.1 | 2.05 |
| | 3 | 0.47 | 2.13 | 3 |
| | 4 | 0.44 | 2.25 | 4.4 |
| | 5 | 0.41 | 2.45 | 6.4 |
| | 6 | 0.37 | 2.7 | 8.8 |
| | 7 | 0.34 | 3 | 11.8 |
| 0.4 | 1 | 0.3 | 3.3 | 2.33 |
| | 2 | 0.32 | 3.12 | 4 |
| | 3 | 0.28 | 3.5 | 6.62 |
| | 4 | 0.26 | 3.9 | 10.5 |
| | 5 | 0.23 | 4.4 | 15.75 |
| | 6 | 0.2 | 5.23 | 22.5 |
| | 7 | 0.17 | 5.9 | 30.8 |

(b) For $P_{on} = 0.2$

| $P_e$ | $N$ | $R_s$ | $T_D$ | $\tau$ |
|---|---|---|---|---|
| 0 | 1 | 0.4 | 2.5 | 1 |
| | 2 | 0.533 | 1.87 | 1 |
| | 3 | 0.6 | 1.66 | 1 |
| | 4 | 0.64 | 1.56 | 1 |
| | 5 | 0.66 | 1.5 | 1 |
| | 6 | 0.68 | 1.45 | 1 |
| | 7 | 0.7 | 1.42 | 1 |
| .2 | 1 | 0.32 | 3.12 | 1.6 |
| | 2 | 0.38 | 2.6 | 2.3 |
| | 3 | 0.37 | 2.63 | 3.5 |
| | 4 | 0.36 | 2.77 | 5.2 |
| | 5 | 0.33 | 3.01 | 7.5 |
| | 6 | 0.3 | 3.25 | 10.3 |
| | 7 | 0.28 | 3.5 | 13.8 |
| 0.4 | 1 | 0.24 | 4.16 | 2.66 |
| | 2 | 0.25 | 3.9 | 4.81 |
| | 3 | 0.23 | 4.35 | 8.1 |
| | 4 | 0.21 | 4.86 | 12.9 |
| | 5 | 0.17 | 5.66 | 19.3 |
| | 6 | 0.15 | 6.39 | 27.5 |
| | 7 | 0.14 | 7.13 | 37.5 |

(c) For $P_{on} = 0.4$

| $P_{on}$ | $N$ | $R_s$ | $T_D$ | $\tau$ |
|---|---|---|---|---|
| 0 | 1 | 0.3 | 3.33 | 1 |
| | 2 | 0.4 | 2.5 | 1 |
| | 3 | 0.45 | 2.2 | 1 |
| | 4 | 0.48 | 2.1 | 1 |
| | 5 | 0.5 | 1 | 1 |
| | 6 | 0.51 | 1.94 | 1 |
| | 7 | 0.52 | 1.9 | 1 |
| 0.2 | 1 | 0.24 | 4.17 | 1.83 |
| | 2 | 0.29 | 3.47 | 2.83 |
| | 3 | 0.28 | 3.5 | 4.33 |
| | 4 | 0.27 | 3.66 | 6.5 |
| | 5 | 0.25 | 3.9 | 9.44 |
| | 6 | 0.24 | 4.2 | 13.1 |
| | 7 | 0.22 | 4.5 | 17.4 |
| 0.4 | 1 | 0.18 | 5.5 | 3.21 |
| | 2 | 0.19 | 5.21 | 6.15 |
| | 3 | 0.17 | 5.76 | 10.62 |
| | 4 | 0.15 | 6.4 | 17.1 |
| | 5 | 0.13 | 7.44 | 25.6 |
| | 6 | 0.12 | 8.38 | 36.4 |
| | 7 | 0.106 | 9.4 | 49.4 |

**TABLE 1. Summary of the variables used for generating both the analytical and simulation results for our CGBN-HARQ scheme, where the results shown are in units of $T_p$ and the sensing duration is $T_p$. The variables $R_S$, $T_D$ and $\tau$ represent the throughput, average packet delay and average end-to-end packet delay. (a) For $P_{on} = 0$. (b) For $P_{on} = 0.2$. (c) For $P_{on} = 0.4$.**

a) The end-to-end packet-delay, such as $mT_p$ of the new packets whose transmission was started during state $S_i$.
b) The probability of transmission $P_{i,j}^{(m)}$ from $\boldsymbol{I}_i$ (i.e., $S_i \in \mathbb{S}_N$) to the different termination states in $\mathbb{S}$.
c) The number of packets $l_{i,j}$ whose transmission was started in state $S_i$ and was correctly received in state $S_j$.

With the aid of the above information, we update $\mathbf{P}_{MF}$ as follows:

$$P(m) \leftarrow P(m-1) + \frac{\pi_i \times l_{i,j} \times P_{i,j}^{(m)}}{L_i}, \quad m = 1, 2 \ldots, M_T, S_i \in S_i^{(m)}, S_i \in \mathbb{S}_N. \quad (26)$$

Having obtained the PMF of the end-to-end packet-delay, the average end-to-end packet-delay can be formulated as

$$\tau = \sum_{i=1}^{M_T} iT_P \times P(i). \quad (27)$$

Let us now characterize the attainable throughput and the delay performance of the CGBN-HARQ system.

## V. PERFORMANCE RESULTS

In this section, we characterize the performance of the CGBN-HARQ. Both analytical and simulation results are provided for confirming each other. The proposed CGBN-HARQ scheme is configured in Matlab, where the CR transmitter is enabled to sense the channel and to continuously transmit $N$ packets in the sensed free TS. On the other hand, the CR receiver detects a packet and performs RS decoding. Fifty thousand Monte Carlo simulations were performed for all the values of $P_{on}, P_{off}$, $P_e$ and $N$. The variables and their performance impacts are summarized in the Table 1. Moreover, the observation period starts from the first TS and continues until all packets were successfully received by the CR receiver.

From our studies in the previous sections, we can see that both the throughput and delay performance are dependent on the following system parameters: the PU's channel utilization probability ($P_{on}$), CU error reliability ($P_e$), the number of packets ($N$) transmitted in a TS and the time $kT_p$ required for reliable sensing. Thus, we will characterize the performance as a function of these parameters. Note that in our simulations the observation period of $N_t$ TSs spans from the first TS until the instant when all $N_s$ packets have been successfully received. From this, the throughput is obtained as

$$R_S = \frac{N_s}{N_t(k+N)} \text{ (packets per } T_p). \quad (28)$$

Note that, $N_t$ includes both the free and the busy TSs encountered during the observation period. Correspondingly, the

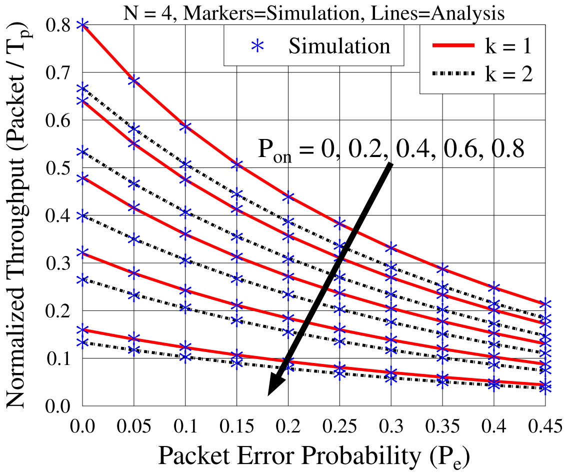


**FIGURE 13.** Throughput performance of the CGBN-HARQ versus packet error probability in terms of various channel busy probabilities, when $k = 1$ or 2, and $N = 4$.

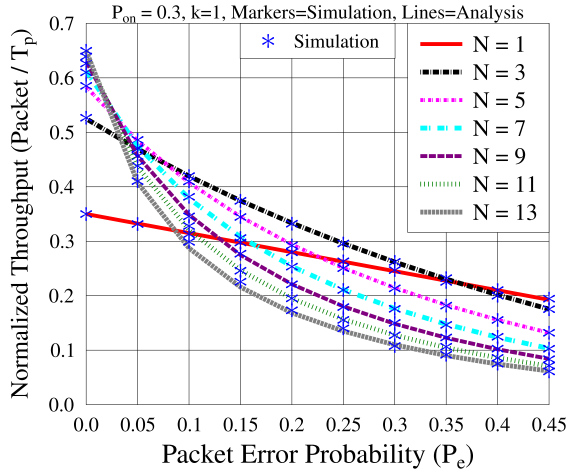


**FIGURE 14.** Throughput performance of the CGBN-HARQ versus packet error probability and for various values of $N$, when $k = 1$ and $P_{on} = 0.3$.

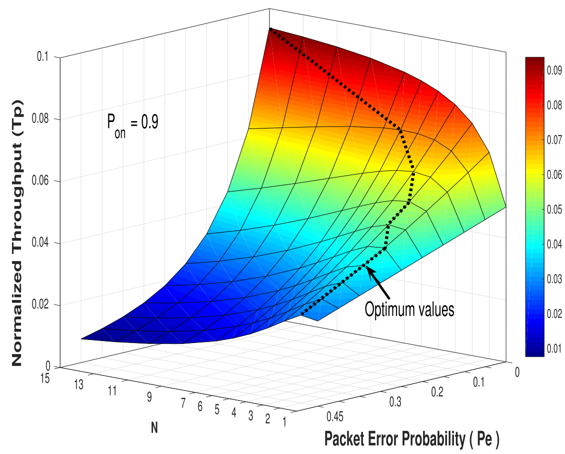


**FIGURE 15.** Throughput performance of the CGBN-HARQ versus packet error probability and various values of $N$, when $k = 1$ and $P_{on} = 0.9$. The optimum values of $N$ which maximize the throughput are shown using *solid* black line.

average packet-delay is given by:

$$T_{DS} = \frac{N_t(k+N)}{N_s} \times T_p \text{ (seconds)} \quad (29)$$

or simply by $T_{DS} = \frac{N_t(k+N)}{N_s}$ in terms of number of $T_p's$ intervals which represent the normalized average packet-delay $T_{DS}$ in units of $T_p$.

Fig. 13 shows the effect of packet error probability on the achievable throughput of CGBN-HARQ for various combinations of $P_{on}$ and $k$. Observe the high degree of agreement between the analytical and simulation results. Explicitly, the throughput decreases as $P_e$ increases due to the increase in the number of packet retransmissions, as $P_e$ increases. For a given $P_e$, the throughput decreases as $P_{on}$ increases, because the CR system is granted less time for its information transmission. Finally, it can also be seen that the throughput is affected by the time used for reliable channel sensing. The throughput is reduced, as the sensing duration increases.

Fig. 14 and 15 show the throughput attained by CGBN-HARQ, when various values of $N$ and $P_e$ are assumed. These figures also show the optimum values of $N$ for each $P_e$ and for the other fixed parameters. It may be concluded from the plots of Fig. 14 and 15 that the optimum values of $N$ maximizing the throughput increases, when the channel becomes more reliable. When comparing Fig. 14 to 15, we observe once again observe that the throughput decreases, when $P_{on}$ increases.

Having characterized the attainable throughput, we now continue by quantifying the delay in terns of both the average packet-delay and the end-to-end packet-delay. Let us first consider the average packet-delay.

Fig. 16 illustrates the effect of $P_e$ on the average packet-delay. It can be observed from Fig. 16 that the average packet-delay increases, when $P_e$ or/and $P_{on}$ increase, when the other system parameters. Explicitly, the average packet-delay increases due to the increased number of retransmissions, when $P_e$ increases. When $P_{on}$ increases, there is a lower probability of finding free TS for transmission by the CR system, hence the average packet-delay increases. As shown in Fig. 16, increasing the sensing duration also increases the average packet-delay owing to the reduced time in each TS used for packet transmission. When comparing Fig. 13 to 16, we can observe the inverse relationship between the attainable throughput and the average packet-delay, as formulated in Equation (18) and (21). Additionally, the simulation results of Fig. 16 agree well with the analytical results.

First, Fig. 17 shows the effect of the number of packets $N$ per TS on the average packet-delay. An interesting trend in the results shown of Fig. 17 is the cross-over between the curves for the different values of $N$. This may be explained as follows. There are two factors contributing to the average packet-delay, namely the sensing time and the retransmission duration imposed by the corrupted transmissions. Increasing the value of $N$ reduces the contribution of the delay due

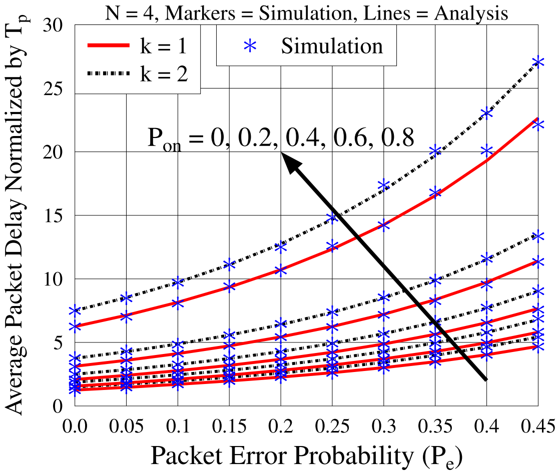


**FIGURE 16.** Average packet-delay of the CGBN-HARQ system versus packet error probability, when $k = 1$ or 2, and $N = 4$.

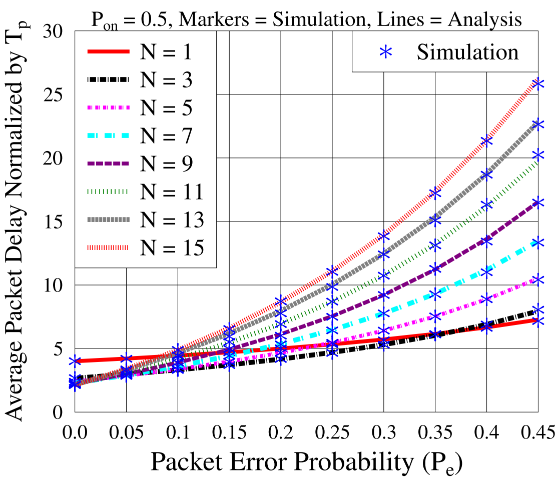


**FIGURE 17.** Average packet-delay of the CGBN-HARQ system versus packet error probability, when $P_{on} = 0.5$ and $k = 1T_p$.

to sensing. For example, for $N = 1$, a single packet is transmitted with a single $T_p$ duration of sensing delay. By contrast, when $N = 15$, as many as 15 packets are transmitted within the same single $T_p$ duration of sensing delay. On the other hand, as $N$ increases, a higher delay is imposed, when a packet has to be retransmitted. Thus, increasing the value of $N$ decreases the relative sensing delay per packet but increases the relative retransmission delay. Naturally, the delay due to the sensing operation only becomes explicit, when the communication channel is very reliable. When the channel becomes less reliable, the delay imposed by retransmissions will dominate the overall packet-delay. Therefore, the average packet-delay decreases with $N$ for low values of $P_e$, while it increases for higher values of $P_e$, hence the curves intersect each other.

Having considered the average packet-delay, we now turn our attention to the end-to-end delay. As discussed earlier in Section IV-C.2, the end-to-end delay is defined as the time

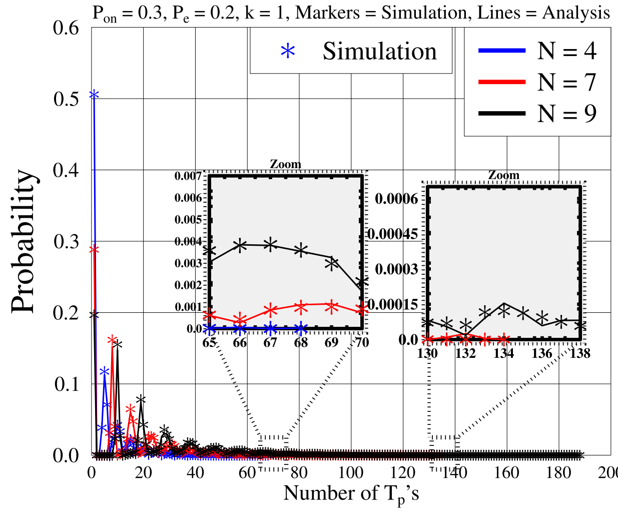


**FIGURE 18.** Probability of end-to-end packet-delay in the CGBN-HARQ systems, when $P_{on} = 0.3$, $P_e = 0.2$, $k = 1$ and $N = 4$, 7 and 9.

duration between the transmission of a packet and its ultimate successful reception. In simulations, the end-to-end packet-delay can be calculated for each packet of say $N_s$ packets that the transmitter is required to transmit. Let us define a vector $\boldsymbol{d}$ of length $N_s$, in which the $j$th element $\boldsymbol{d}(j)$ is the end-to-end delay of the $j$th packet. Then, the PMF of the end-to-end packet-delay may be formulated as:

$$P(i) = \frac{\sum_{j=1}^{N_s} \delta\left(d(j) - i\right)}{N_s}, \quad 1 \leq i \leq \max(\boldsymbol{d}). \tag{30}$$

where $\max(\boldsymbol{d})$ denotes the maximum delay of the $N_s$ packets.

Fig. 18 shows the probability distribution of the end-to-end packet-delay of the proposed CGBN-HARQ scheme. It can be observed from Fig. 18 that for the case of $N = 4$, 50.59% of packets are received successfully in the first instance of transmission (i.e. within an end-to-end delay of a single $T_p$), 3.86% packet are received successfully with an end-to-end delay of $4T_p$, and 1.56% packets are received successfully with an end-to-end delay of $14T_p$. Similarly, the probability distributions can be evaluated for the scenarios of $N = 7$ and $N = 9$ by either simulations or based on the analytical results of Section IV-C.2. It can be seen from Fig. 18 that the simulation results agree well with the analytical ones. Furthermore, the length of the tail increases, as the value of $N$ increases, implying that the maximum possible delay increases, when $N$ increases.

Fig. 19 shows the average end-to-end packet-delay versus $P_e$ with respect to different values of $P_{on}$. In the figure, the values obtained from simulations are calculated according to:

$$\tau_s = \sum_{i=1}^{\max(\boldsymbol{d})} \mathbf{P}_{ds}(i) \times i \ \ (T_p\text{'s}). \tag{31}$$

It can be seen from Fig. 19 that the average end-to-end packet-delay explicitly increases, as $P_e$ increases because of the

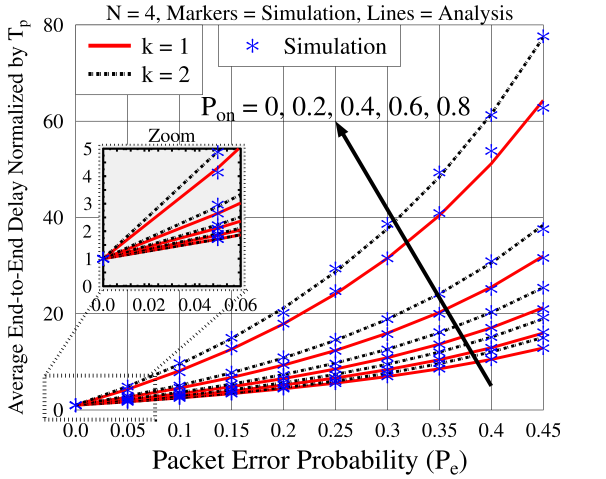


**FIGURE 19.** Average end-to-end packet-delay of the CGBN-HARQ versus packet error probability for various values of $P_{on}$, when $N = 4$ and $k = 1$ or 2.

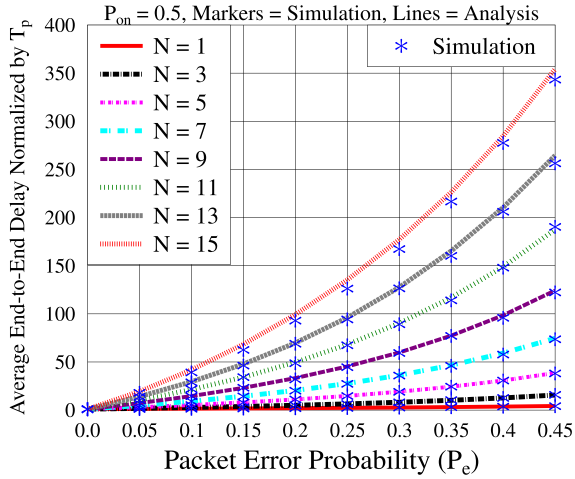


**FIGURE 20.** Average end-to-end packet-delay of the CGBN-HARQ versus packet error probability for various values of $N$, when $P_{on} = 0.5$ and $k = 1$.

increase in the number of retransmission. The average end-to-end packet-delay also increases, when $P_{on}$ increases, because the CU has to wait for longer to acquire a free TS.

When comparing Fig. 16 and 19, there are two striking differences. The first difference concerns the minimum values of both the delays, while the second difference concerns the increasing rates of the delays, as $P_e$ or/and $P_{on}$ increases. In more detail, firstly, as depicted in Fig. 19, the minimum end-to-end packet-delay equals to one for $P_e = 0$, regardless of the value of $P_{on}$. However, in the case of the average packet-delay, as shown Fig. 16, the minimum value becomes higher than one and increases as $P_{on}$ increases. This is because, unlike the average packet-delay, which is calculated by averaging the observations over $N_t$ TSs, the end-to-end packet-delay is individually calculated for each packet from the start of their transmission. In other words, when $P_e = 0$, the average packet-delay includes the sensing delay, the delay due to the PU channel being busy, as well as owing to the transmission delay of one $T_p$. On the other hand, when $P_e = 0$, the average *end-to-end* packet-delay always equals one $T_p$, because the error-free channel ensures the correct delivery of a transmitted packet during the first attempt. Secondly, when comparing Fig. 19 to Fig. 16, we can find that the average end-to-end packet-delay increases significantly faster than the average packet delay, when $P_e$ or/and $P_{on}$ increases. This is because in the CGBN-HARQ every packet transmitted is dependent on the $(N-1)$ packets transmitted in the front of it. Explicitly, if any of these packets is received in error, the packet considered has to be retransmitted, regardless whether it has or has not been correctly received, thereby resulting in a longer end-to-end packet-delay.

Finally, in Fig. 20, we show the effect of increasing $N$ on the average end-to-end packet-delay, where for the reason mentioned above, the average end-to-end delay has a minimum value of one at $P_e = 0$, regardless of the value of $N$. Explicitly, at a given $P_e$, the average end-to-end delay increases, as the value of $N$ becomes higher.

## VI. CONCLUSION

We proposed a CGBN-HARQ transmission scheme for a CR system with the objective of improving the attainable bandwidth efficiency, while maintaining reliable data transmission. Our investigations have included both its mathematical analysis and simulations. The analytical study of the proposed scheme has relied on the CR system being modelled using a discrete-time Markov chain. The results obtained for this system model include an algorithm conceived for generating all possible states of the CR transmitter. We have also derived closed-form expressions for the throughput and delay of the CGBN-HARQ scheme. The analytical results have also been confirmed by simulations. Specifically, the performance results demonstrated that both the throughput and the delay of the proposed system is significantly affected by the PU's activities and by the PU's channel quality. The results shows a significant increase in the transmission delay owing to less reliable communication and/or due to the increase in the channel occupancy by the PUs. Moreover, we also investigated the impact of transmitting various number of packets on both the achievable throughput and on the transmission delay. It was demonstrated that in order to achieve the maximum attainable throughput and minimum delay, the number of packet transmission in a TS should be carefully adopted according to the communication environment. The summarized results of the CGBN-HARQ are presented in the Table 1. Our future research will focus on extending this work for finding the optimal transmission frame length.

## VII. Acknowledgement

This paper was presented at the IEEE Vehicular Technology Conference, Nanjing, China, May 2016.

## REFERENCES

[1] E. Hossain, D. Niyato, and Z. Han, *Dynamic Spectrum Access and Management in Cognitive Radio Networks*. Cambridge, U.K.: Cambridge Univ. Press, 2009.

[2] G. Staple and K. Werbach, "The end of spectrum scarcity [spectrum allocation and utilization]," *IEEE Spectr.*, vol. 41, no. 3, pp. 48–52, Mar. 2004.

[3] *Spectrum Policy Task Force Report Technical Report*, document ET Docket 02-155, FCC, Washington, DC, USA, Nov. 2002.

[4] *Notice of Proposed Rule Making and Order*, document ET Docket 03-222, Dec. 2003.

[5] M. A. McHenry, P. A. Tenhula, D. McCloskey, D. A. Roberson, and C. S. Hood, "Chicago spectrum occupancy measurements & analysis and a long-term studies proposal," in *Proc. 1st Int. Workshop Technol. Policy Accessing Spectr. (TAPAS)*, Aug. 2006, Art. no. 1.

[6] J. Yang, "Spatial channel characterization for cognitive radios," Dept. EECS, Univ. California Berkeley, Berkeley, CA, USA, Tech. Rep. UCB/ERL M05/8, Jan. 2005. [Online]. Available: http://www.eecs.berkeley.edu/Pubs/TechRpts/2005/4293.html

[7] D. Cabric, "Cognitive radios: System design perspective," Ph.D. dissertation, Dept. Electron. Comput. Sci., Univ. California Berkeley, Berkeley, CA, USA, 2007.

[8] M. H. Islam *et al.*, "Spectrum survey in Singapore: Occupancy measurements and analyses," in *Proc. 3rd Int. Conf. Cognit. Radio Oriented Wireless Netw. Commun. (CrownCom)*, May 2008, pp. 1–7.

[9] Q. Zhao and B. M. Sadler, "A survey of dynamic spectrum access," *IEEE Signal Process. Mag.*, vol. 24, no. 3, pp. 79–89, May 2007.

[10] I. F. Akyildiz, W.-Y. Lee, M. C. Vuran, and S. Mohanty, "Next generation/dynamic spectrum access/cognitive radio wireless networks: A survey," *Comput. Netw.*, vol. 50, no. 13, pp. 2127–2159, Sep. 2006.

[11] F. Akhtar, M. H. Rehmani, and M. Reisslein, "White space: Definitional perspectives and their role in exploiting spectrum opportunities," *Telecommun. Policy*, vol. 40, no. 4, pp. 319–331, Apr. 2016.

[12] J. Mitola and G. Q. Maguire, Jr., "Cognitive radio: Making software radios more personal," *IEEE Pers. Commun.*, vol. 6, no. 4, pp. 13–18, Apr. 1999.

[13] S. Haykin, "Cognitive radio: Brain-empowered wireless communications," *IEEE J. Sel. Areas Commun.*, vol. 23, no. 2, pp. 201–220, Feb. 2005.

[14] D. Cabric, S. M. Mishra, and R. W. Brodersen, "Implementation issues in spectrum sensing for cognitive radios," in *Proc. Conf. Rec. 38th Asilomar Conf. Signals, Syst. Comput.*, vol. 1. Nov. 2004, pp. 772–776.

[15] G. Ganesan and Y. Li, "Cooperative spectrum sensing in cognitive radio, part I: Two user networks," *IEEE Trans. Wireless Commun.*, vol. 6, no. 6, pp. 2204–2213, Jun. 2007.

[16] T. Yucek and H. Arslan, "A survey of spectrum sensing algorithms for cognitive radio applications," *IEEE Commun. Surveys Tuts.*, vol. 11, no. 1, pp. 116–130, 1st Quart., 2009.

[17] E. Axell, G. Leus, E. G. Larsson, and H. V. Poor, "Spectrum sensing for cognitive radio: State-of-the-art and recent advances," *IEEE Signal Process. Mag.*, vol. 29, no. 3, pp. 101–116, May 2012.

[18] *IEEE Recommended Practice for Information Technology-Telecommunications and Information Exchange Between Systems Wireless Regional Area Networks (WRAN)-Specific Requirements—Part 22.2: Installation and Deployment of IEEE 802.22 Systems*, IEEE Standard 802.22.2-2012, Sep. 2012, pp. 1–44.

[19] Y. Xiao and F. Hu, *Cognitive Radio Networks*. New York, NY, USA: Auerbach, Jan. 2009.

[20] Y.-C. Liang, Y. Zeng, E. C. Y. Peh, and A. T. Hoang, "Sensing-throughput tradeoff for cognitive radio networks," *IEEE Trans. Wireless Commun.*, vol. 7, no. 4, pp. 1326–1337, Apr. 2008.

[21] H. Su and X. Zhang, "Cross-layer based opportunistic MAC protocols for QoS provisionings over cognitive radio wireless networks," *IEEE J. Sel. Areas Commun.*, vol. 26, no. 1, pp. 118–129, Jan. 2008.

[22] X. Hong, J. Wang, C.-X. Wang, and J. Shi, "Cognitive radio in 5G: A perspective on energy-spectral efficiency trade-off," *IEEE Commun. Mag.*, vol. 52, no. 7, pp. 46–53, Jul. 2014.

[23] W. Y. Lee and I. F. Akyildiz, "Optimal spectrum sensing framework for cognitive radio networks," *IEEE Trans. Wireless Commun.*, vol. 7, no. 10, pp. 3845–3857, Oct. 2008.

[24] S. Akin and M. C. Gursoy, "Performance analysis of cognitive radio systems under QoS constraints and channel uncertainty," *IEEE Trans. Wireless Commun.*, vol. 10, no. 9, pp. 2883–2895, Sep. 2011.

[25] Y. Saleem and M. H. Rehmani, "Primary radio user activity models for cognitive radio networks: A survey," *J. Netw. Comput. Appl.*, vol. 43, pp. 1–16, Aug. 2014.

[26] X. Kang, Y. C. Liang, H. K. Garg, and L. Zhang, "Sensing-based spectrum sharing in cognitive radio networks," *IEEE Trans. Veh. Technol.*, vol. 58, no. 8, pp. 4649–4654, Oct. 2009.

[27] S. Stotas and A. Nallanathan, "Enhancing the capacity of spectrum sharing cognitive radio networks," *IEEE Trans. Veh. Technol.*, vol. 60, no. 8, pp. 3768–3779, Oct. 2011.

[28] S. Lin and D. J. Costello, *Error Control Coding: Fundamentals and Applications*, 2nd ed. Upper Saddle River, NJ, USA: Prentice-Hall, 1999.

[29] D. Bertsekas and R. Gallagher, *Data Networks*, 2nd ed. Englewood Cliffs, NJ, USA: Prentice Hall, 1991.

[30] A. Leon-Garcia and I. Widjaja, *Communication Networks*. New York, NY, USA: McGraw-Hill, 2004.

[31] Y.-C. Liang, K.-C. Chen, G. Y. Li, and P. Mahonen, "Cognitive radio networking and communications: An overview," *IEEE Trans. Veh. Technol.*, vol. 60, no. 7, pp. 3386–3407, Sep. 2011.

[32] C. Cormio and K. R. Chowdhury, "A survey on MAC protocols for cognitive radio networks," *Ad Hoc Netw.*, vol. 7, no. 7, pp. 1315–1329, Sep. 2009.

[33] A. De Domenico, E. Strinati, and M.-G. Di Benedetto, "A survey on MAC strategies for cognitive radio networks," *IEEE Commun. Surveys Tut.*., vol. 14, no. 1, pp. 21–44, 1st Quart., 2012.

[34] L. Hanzo, T. Liew, B. Yeap, R. Tee, and S. X. Ng, *Turbo Coding, Turbo Equalisation and Space-Time Coding: EXIT-Chartaided Near-Capacity Designs for Wireless Channels*, 2nd ed. Hoboken, NJ, USA: Wiley, 2011.

[35] J. M. Wozencraft and M. Horstein, "Coding for two-way channels," presented at the 4th London Symp. Inf. Theory, London, U.K., Aug./Sep. 1960, pp. 1–16. [Online]. Available: http://dspace.mit.edu/bitstream/handle/1721.1/4439/RLE-TR-383-04741026.pdf;sequence=1

[36] S. Lin, D. J. Costello, and M. J. Miller, "Automatic-repeat-reQuest error-control schemes," *IEEE Commun. Mag.*, vol. 22, no. 12, pp. 5–17, Dec. 1984.

[37] J. Du, M. Kasahara, and T. Namekawa, "Separate codes on type-II hybrid ARQ systems," *IEEE Trans. Commun.*, vol. 36, no. 10, pp. 1089–1097, Oct. 1988.

[38] S. Kallel, "Analysis of a type II hybrid ARQ scheme with code combining," *IEEE Trans. Commun.*, vol. 38, no. 8, pp. 1133–1137, Aug. 1990.

[39] P. Decker, "An adaptive type-II hybrid ARQ/FEC protocol suitable for GSM," in *Proc. IEEE 44th Veh. Technol. Conf.*, vol. 1. Jun. 1994, pp. 330–333.

[40] H. Liu and M. El Zarki, "Performance of H.263 video transmission over wireless channels using hybrid ARQ," *IEEE J. Sel. Areas Commun.*, vol. 15, no. 9, pp. 1775–1786, Dec. 1997.

[41] J. Hamorsky and L. Hanzo, "Performance of the turbo hybrid automatic repeat reQuest system type II," in *Proc. Inf. Theory Netw. Workshop*, Jun. 1999, p. 51.

[42] E. M. Sozer, M. Stojanovic, and J. G. Proakis, "Underwater acoustic networks," *IEEE J. Ocean. Eng.*, vol. 25, no. 1, pp. 72–83, Jan. 2000.

[43] G. Caire and D. Tuninetti, "The throughput of hybrid-ARQ protocols for the Gaussian collision channel," *IEEE Trans. Inf. Theory*, vol. 47, no. 5, pp. 1971–1988, Jul. 2001.

[44] W. T. Kim, S. J. Bae, J. G. Kim, and E. K. Joo, "Performance of STBC with turbo code in HARQ scheme for mobile communication systems," in *Proc. 10th Int. Conf. Telecommun. (ICT)*, vol. 1. Feb. 2003, pp. 85–89.

[45] B. Zhao and M. C. Valenti, "Practical relay networks: A generalization of hybrid-ARQ," *IEEE J. Sel. Areas Commun.*, vol. 23, no. 1, pp. 7–18, Jan. 2005.

[46] K. C. Beh, A. Doufexi, and S. Armour, "Performance evaluation of hybrid ARQ schemes of 3GPP LTE OFDMA system," in *Proc. IEEE 18th Int. Symp. Pers., Indoor Mobile Radio Commun.*, Sep. 2007, pp. 1–5.

[47] M. C. Vuran and I. F. Akyildiz, "Error control in wireless sensor networks: A cross layer analysis," *IEEE/ACM Trans. Netw.*, vol. 17, no. 4, pp. 1186–1199, Aug. 2009.

[48] R. Zhang and L. Hanzo, "Superposition-aided delay-constrained hybrid automatic repeat reQuest," *IEEE Trans. Veh. Technol.*, vol. 59, no. 4, pp. 2109–2115, May 2010.

[49] R. Zhang and L. Hanzo, "A unified treatment of superposition coding aided communications: Theory and practice," *IEEE Commun. Surveys Tut.*, vol. 13, no. 3, pp. 503–520, 3rd Quart., 2011.

[50] H. Chen, R. G. Maunder, and L. Hanzo, "Low-complexity multiple-component turbo-decoding-aided hybrid ARQ," *IEEE Trans. Veh. Technol.*, vol. 60, no. 4, pp. 1571–1577, May 2011.

[51] H. Chen, R. G. Maunder, and L. Hanzo, "Lookup-table-based deferred-iteration aided low-complexity turbo hybrid ARQ," *IEEE Trans. Veh. Technol.*, vol. 60, no. 7, pp. 3045–3053, Sep. 2011.

[52] H. Chen, R. G. Maunder, and L. Hanzo, "Deferred-iteration aided low-complexity turbo hybrid ARQ relying on a look-up table," in *Proc. IEEE Global Telecommun. Conf. (GLOBECOM)*, Dec. 2011, pp. 1–5.

[53] H. Chen, R. G. Maunder, and L. Hanzo, "A survey and tutorial on low-complexity turbo coding techniques and a holistic hybrid ARQ design example," *IEEE Commun. Surveys Tuts.*, vol. 15, no. 4, pp. 1546–1566, 4th Quart., 2013.

[54] B. Zhang, H. Chen, M. El-Hajjar, R. Maunder, and L. Hanzo, "Distributed multiple-component turbo codes for cooperative hybrid ARQ," *IEEE Signal Process. Lett.*, vol. 20, no. 6, pp. 599–602, Jun. 2013.

[55] K. Xu *et al.*, "NTC-HARQ: NetworkŰturbo-coding based HARQ protocol for wireless broadcasting system," *IEEE Trans. Veh. Technol.*, vol. 64, no. 10, pp. 4633–4644, Oct. 2015.

[56] N. D. K. Liyanage, C. A. Abeywickrama, P. M. I. U. Kumari, S. A. D. Silva, and C. B. Wavegedara, "Performance investigation of hybrid ARQ in HSDPA systems with AMC," in *Proc. Moratuwa Eng. Res. Conf. (MERCon)*, Apr. 2016, pp. 126–131.

[57] C. Zhu, Y. Huo, B. Zhang, R. Zhang, M. El-Hajjar, and L. Hanzo, "Adaptive-truncated-HARQ-aided layered video streaming relying on interlayer FEC coding," *IEEE Trans. Veh. Technol.*, vol. 65, no. 3, pp. 1506–1521, Mar. 2016.

[58] R. E. Ramos and K. Madani, "A novel generic distributed intelligent re-configurable mobile network architecture," in *Proc. 53rd IEEE Veh. Technol. Conf. (VTC)*, vol. 3. May 2001, pp. 1927–1931.

[59] D. Cabric and R. W. Brodersen, "Physical layer design issues unique to cognitive radio systems," in *Proc. IEEE 16th Int. Symp. Pers. Indoor Mobile Radio Commun. (PIMRC)*, vol. 2. Sep. 2005, pp. 759–763.

[60] N. Devroye, P. Mitran, and V. Tarokh, "Limits on communications in a cognitive radio channel," *IEEE Commun. Mag.*, vol. 44, no. 6, pp. 44–49, Jun. 2006.

[61] A. Baker, S. Ghosh, A. Kumar, and M. Bayoumi, "Notice of violation of IEEE publication principles LDPC decoder: A cognitive radio perspective for next generation (XG) communication," *IEEE Circuits Syst. Mag.*, vol. 7, no. 3, pp. 24–37, 3rd Quart., 2007.

[62] G. Yue, "Antijamming coding techniques," *IEEE Signal Process. Mag.*, vol. 25, no. 6, pp. 35–45, Nov. 2008.

[63] K. B. Letaief and W. Zhang, "Cooperative communications for cognitive radio networks," *Proc. IEEE*, vol. 97, no. 5, pp. 878–893, May 2009.

[64] G. Yue and X. Wang, "Anti-jamming coding techniques with application to cognitive radio," *IEEE Trans. Wireless Commun.*, vol. 8, no. 12, pp. 5996–6007, Dec. 2009.

[65] R. A. Roshid, N. M. Aripin, N. Fisal, S. H. S. Ariffin, and S. K. S. Yusof, "Integration of cooperative sensing and transmission," *IEEE Veh. Technol. Mag.*, vol. 5, no. 3, pp. 46–53, Sep. 2010.

[66] S.-M. Cheng, W. C. Ao, and K.-C. Chen, "Efficiency of a cognitive radio link with opportunistic interference mitigation," *IEEE Trans. Wireless Commun.*, vol. 10, no. 6, pp. 1715–1720, Jun. 2011.

[67] B. Makki, A. G. I. Amat, and T. Eriksson, "HARQ feedback in spectrum sharing networks," *IEEE Commun. Lett.*, vol. 16, no. 9, pp. 1337–1340, Sep. 2012.

[68] Y. Yang, H. Ma, and S. Aissa, "Cross-layer combining of adaptive modulation and truncated ARQ under cognitive radio resource requirements," *IEEE Trans. Veh. Technol.*, vol. 61, no. 9, pp. 4020–4030, Nov. 2012.

[69] R. Andreotti, I. Stupia, V. Lottici, F. Giannetti, and L. Vandendorpe, "Goodput-based link resource adaptation for reliable packet transmissions in BIC-OFDM cognitive radio networks," *IEEE Trans. Signal Process.*, vol. 61, no. 9, pp. 2267–2281, May 2013.

[70] J. S. Harsini and M. Zorzi, "Transmission strategy design in cognitive radio systems with primary ARQ control and QoS provisioning," *IEEE Trans. Commun.*, vol. 62, no. 6, pp. 1790–1802, Jun. 2014.

[71] Y.-C. Chen, I.-W. Lai, K.-C. Chen, W.-T. Chen, and C.-H. Lee, "Transmission latency and reliability trade-off in path-time coded cognitive radio ad hoc networks," in *Proc. IEEE Global Commun. Conf.*, Dec. 2014, pp. 1084–1089.

[72] J. Li, T. Luo, J. Gao, and G. Yue, "A MAC protocol for link maintenance in multichannel cognitive radio ad hoc networks," *J. Commun. Netw.*, vol. 17, no. 2, pp. 172–183, Apr. 2015.

[73] B. Makki, T. Svensson, and M. Zorzi, "Finite block-length analysis of spectrum sharing networks: Interference-constrained scenario," *IEEE Wireless Commun. Lett.*, vol. 4, no. 4, pp. 433–436, Aug. 2015.

[74] B. Makki, T. Svensson, and M. Zorzi, "Finite block-length analysis of spectrum sharing networks using rate adaptation," *IEEE Trans. Commun.*, vol. 63, no. 8, pp. 2823–2835, Aug. 2015.

[75] S. H. R. Bukhari, M. H. Rehmani, and S. Siraj, "A survey of channel bonding for wireless networks and guidelines of channel bonding for futuristic cognitive radio sensor networks," *IEEE Commun. Surveys Tuts.*, vol. 18, no. 2, pp. 924–948, 2nd Quart., 2016. [Online]. Available: http://dx.doi.org/10.1109/COMST.2015.2504408

[76] D. W. K. Ng, E. S. Lo, and R. Schober, "Multiobjective resource allocation for secure communication in cognitive radio networks with wireless information and power transfer," *IEEE Trans. Veh. Technol.*, vol. 65, no. 5, pp. 3166–3184, May 2016.

[77] K. Sohrabi, J. Gao, V. Ailawadhi, and G. J. Pottie, "Protocols for self-organization of a wireless sensor network," *IEEE Pers. Commun.*, vol. 7, no. 5, pp. 16–27, Oct. 2000.

[78] E. Buracchini, "The software radio concept," *IEEE Commun. Mag.*, vol. 38, no. 9, pp. 138–143, Sep. 2000.

[79] A. He *et al.*, "Development of a case-based reasoning cognitive engine for IEEE 802.22 WRAN applications," *ACM SIGMOBILE Mobile Comput. Commun. Rev.*, vol. 13, no. 2, pp. 37–48, Apr. 2009.

[80] I. F. Akyildiz, W.-Y. Lee, M. C. Vuran, and S. Mohanty, "A survey on spectrum management in cognitive radio networks," *IEEE Commun. Mag.*, vol. 46, no. 4, pp. 40–48, Apr. 2008.

[81] *Second Report and Order*, document ET Docket 08-260, FCC, Washington, DC, USA, Nov. 2008.

[82] O. B. Akan, O. Karli, and O. Ergul, "Cognitive radio sensor networks," *IEEE Netw.*, vol. 23, no. 4, pp. 34–40, Jul./Aug. 2009.

[83] I. F. Akyildiz, W. Y. Lee, and K. R. Chowdhury, "CRAHNs: Cognitive radio ad hoc networks," *Ad Hoc Netw.*, vol. 7, pp. 810–836, Jul. 2009.

[84] A. O. Bicen and O. B. Akan, "Reliability and congestion control in cognitive radio sensor networks," *Ad Hoc Netw.*, vol. 9, no. 7, pp. 1154–1164, Sep. 2011.

[85] A. O. Bicen, V. C. Gungor, and O. B. Akan, "Delay-sensitive and multimedia communication in cognitive radio sensor networks," *Ad Hoc Netw.*, vol. 10, no. 5, pp. 816–830, Jul. 2012.

[86] G. Ozcan and M. C. Gursoy, "Throughput of cognitive radio systems with finite blocklength codes," *IEEE J. Sel. Areas Commun.*, vol. 31, no. 11, pp. 2541–2554, Nov. 2013.

[87] W. Tang, M. Z. Shakir, M. A. Imran, R. Tafazolli, and M. S. Alouini, "Throughput analysis for cognitive radio networks with multiple primary users and imperfect spectrum sensing," *IET Commun.*, vol. 6, no. 17, pp. 2787–2795, Nov. 2012.

[88] H. Jianhua, K. R. Subramanian, Y. ZongKai, and C. Wenqing, "Analysis of a new broadcast protocol for satellite communications," *IEEE Commun. Lett.*, vol. 4, no. 12, pp. 423–425, Dec. 2000.

[89] P. Chou, A. Mohr, A. Wang, and S. Mehrotra, "Error control for receiver-driven layered multicast of audio and video," *IEEE Trans. Multimedia*, vol. 3, no. 1, pp. 108–122, Mar. 2001.

[90] *IEEE Standard for Local and Metropolitan Area Networks Part 20: Air Interface for Mobile Broadband Wireless Access Systems Supporting Vehicular Mobility—Physical and Media Access Control Layer Specification*, IEEE Standard 802.20-2008, Aug. 2008, pp. 1–1039.

[91] *IEEE Standard for Local and Metropolitan Area Networks Part 16: Air Interface for Broadband Wireless Access Systems Amendment 3: Advanced Air Interface*, IEEE Standard 802.16m-2011 (Amendment to IEEE Standard 802.16-2009), May 2011, pp. 1–1112.

[92] *IEEE Standard for Wireless Man-Advanced Air Interface for Broadband Wireless Access Systems*, IEEE Standard 802.16.1-2012, Sep. 2012, pp. 1–1090.

[93] H. A. Ngo and L. Hanzo, "Hybrid automatic-repeat-reQuest systems for cooperative wireless communications," *IEEE Commun. Surveys Tut.*, vol. 16, no. 1, pp. 25–45, 1st Quart., 2014.

[94] Y. Hayashida and M. Komatsu, "Delay performance of Go-back-N ARQ scheme with Markovian error channel," in *Proc. 2nd Int. Conf. Pers. Commun., Gateway 21st Century*, vol. 1. Oct. 1993, pp. 448–452.

[95] M. Zorzi and R. Rao, "Performance of ARQ Go-Back-N protocol in Markov channels with unreliable feedback: Delay analysis," in *Proc. IEEE 4th Int. Conf. Universal Pers. Commun.*, Nov. 1995, pp. 481–485.

[96] W. Turin, "Throughput analysis of the go-back-N protocol in fading radio channels," *IEEE J. Sel. Areas Commun.*, vol. 17, no. 5, pp. 881–887, May 1999.

[97] S. S. Chakraborty and M. Liinaharja, "On the performance of an adaptive GBN scheme in a time-varying channel," *IEEE Commun. Lett.*, vol. 4, no. 4, pp. 143–145, Apr. 2000.
[98] M. Zorzi, "Some results on error control for burst-error channels under delay constraints," *IEEE Trans. Veh. Technol.*, vol. 50, no. 1, pp. 12–24, Jan. 2001.
[99] K. Ausavapattanakun and A. Nosratinia, "Analysis of Go-Back-N ARQ in block fading channels," *IEEE Trans. Wireless Commun.*, vol. 6, no. 8, pp. 2793–2797, Aug. 2007.
[100] C. Dong, L.-L. Yang, J. Zuo, S. X. Ng, and L. Hanzo, "Energy, delay, and outage analysis of a buffer-aided three-node network relying on opportunistic routing," *IEEE Trans. Commun.*, vol. 63, no. 3, pp. 667–682, Mar. 2015.
[101] C. Dong, L.-L. Yang, and L. Hanzo, "Performance of buffer-aided adaptive modulation in multihop communications," *IEEE Trans. Commun.*, vol. 63, no. 10, pp. 3537–3552, Oct. 2015.
[102] J. C. F. Li, W. Zhang, A. Nosratinia, and J. Yuan, "SHARP: Spectrum harvesting with ARQ retransmission and probing in cognitive radio," *IEEE Trans. Commun.*, vol. 61, no. 3, pp. 951–960, Mar. 2013.
[103] D. Hamza and S. Aissa, "Enhanced primary and secondary performance through cognitive relaying and leveraging primary feedback," *IEEE Trans. Veh. Technol.*, vol. 63, no. 5, pp. 2236–2247, Jun. 2014.
[104] W.-C. Ao and K.-C. Chen, "End-to-end HARQ in cognitive radio networks," in *Proc. IEEE Wireless Commun. Netw. Conf. (WCNC)*, Apr. 2010, pp. 1–6.
[105] S. Touati, H. Boujemaa, and N. Abed, "Cooperative ARQ protocols for underlay cognitive radio networks," in *Proc. 21st Eur. Signal Process. Conf. (EUSIPCO)*, Sep. 2013, pp. 1–5.
[106] G. Yue, X. Wang, and M. Madihian, "Design of anti-jamming coding for cognitive radio," in *Proc. IEEE Global Telecommun. Conf.*, Nov. 2007, pp. 4190–4194.
[107] G. Yue and X. Wang, "Design of efficient ARQ schemes with anti-jamming coding for cognitive radios," in *Proc. IEEE Wireless Commun. Netw. Conf. (WCNC)*, Apr. 2009, pp. 1–6.
[108] Y. Liu, Z. Feng, and P. Zhang, "A novel ARQ scheme based on network coding theory in cognitive radio networks," in *Proc. IEEE Int. Conf. Wireless Inf. Technol. Syst. (ICWITS)*, Aug. 2010, pp. 1–4.
[109] W. Liang, S. X. Ng, J. Feng, and L. Hanzo, "Pragmatic distributed algorithm for spectral access in cooperative cognitive radio networks," *IEEE Trans. Commun.*, vol. 62, no. 4, pp. 1188–1200, Apr. 2014.
[110] J. Hu, L. L. Yang, and L. Hanzo, "Maximum average service rate and optimal queue scheduling of delay-constrained hybrid cognitive radio in Nakagami fading channels," *IEEE Trans. Veh. Technol.*, vol. 62, no. 5, pp. 2220–2229, Jun. 2013.
[111] T. Fujii, Y. Kamiya, and Y. Suzuki, "Multi-band ad-hoc cognitive radio for reducing inter system interference," in *Proc. IEEE 17th Int. Symp. Pers., Indoor Mobile Radio Commun.*, Sep. 2006, pp. 1–5.
[112] S.-L. Cheng and Z. Yang, "Cross-layer combining of power control and adaptive modulation with truncated ARQ for cognitive radios," *J. China Univ. Posts Telecommun.*, vol. 15, no. 3, pp. 19–23, Sep. 2008.
[113] S. Y. Jeon and D. H. Cho, "An ARQ mechanism considering resource and traffic priorities in cognitive radio systems," *IEEE Commun. Lett.*, vol. 13, no. 7, pp. 504–506, Jul. 2009.
[114] A. Ahmad, S. Ahmad, M. H. Rehmani, and N. Ul Hassan, "A survey on radio resource allocation in cognitive radio sensor networks," *IEEE Commun. Surveys Tuts.*, vol. 17, no. 2, pp. 888–917, 2nd Quart., 2015.
[115] W. Liang, H. V. Nguyen, S. X. Ng, and L. Hanzo, "Adaptive-TTCM-aided near-instantaneously adaptive dynamic network coding for cooperative cognitive radio networks," *IEEE Trans. Veh. Technol.*, vol. 65, no. 3, pp. 1314–1325, Mar. 2016.
[116] A. Patel, M. Z. A. Khan, S. N. Merchant, U. B. Desai, and L. Hanzo, "Achievable rates of underlay-based cognitive radio operating under rate limitation," *IEEE Trans. Veh. Technol.*, vol. 65, no. 9, pp. 7149–7159, Sep. 2016.
[117] A. Patel, Z. Khan, S. Merchant, U. Desai, and L. Hanzo, "The achievable rate of interweave cognitive radio in the face of sensing errors," *IEEE Access*, to be published.
[118] Y. Zou, J. Zhu, L. Yang, Y.-C. Liang, and Y.-D. Yao, "Securing physical-layer communications for cognitive radio networks," *IEEE Commun. Mag.*, vol. 53, no. 9, pp. 48–54, Sep. 2015.
[119] A. A. Khan, M. H. Rehmani, and M. Reisslein, "Cognitive radio for smart grids: Survey of architectures, spectrum sensing mechanisms, and networking protocols," *IEEE Commun. Surveys Tuts.*, vol. 18, no. 1, pp. 860–898, Oct. 2016.
[120] A. U. Rehman, L.-L. Yang, and L. Hanzo, "Performance of cognitive hybrid automatic repeat reQuest: Stop-and-wait," in *Proc. IEEE 81st Veh. Technol. Conf. (VTC)*, May 2015, pp. 1–5.
[121] A. U. Rehman, C. Dong, L.-L. Yang, and L. Hanzo, "Performance of cognitive stop-and-wait hybrid automatic repeat reQuest in the face of imperfect sensing," *IEEE Access*, vol. 4, pp. 5489–5508, Jul. 2016.
[122] A. U. Rehman, L. L. Yang, and L. Hanzo, " Performance of cognitive hybrid automatic repeat reQuest: Go-Back-N," in *Proc. IEEE 83rd Veh. Technol. Conf. (VTC)*, May 2016, pp. 1–5.
[123] R. Fantacci, "Queuing analysis of the selective repeat automatic repeat reQuest protocol wireless packet networks," *IEEE Trans. Veh. Technol.*, vol. 45, no. 2, pp. 258–264, May 1996.
[124] L. Badia, M. Rossi, and M. Zorzi, "SR ARQ packet delay statistics on Markov channels in the presence of variable arrival rate," *IEEE Trans. Wireless Commun.*, vol. 5, no. 7, pp. 1639–1644, Jul. 2006.
[125] H. Song, J.-P. Hong, and W. Choi, "On the optimal switching probability for a hybrid cognitive radio system," *IEEE Trans. Wireless Commun.*, vol. 12, no. 4, pp. 1594–1605, Apr. 2013.
[126] R. Howard, *Dynamic Probabilistic Systems: Markov Models*. New York, NY, USA: Wiley, 1971.
[127] R. A. Horn and C. R. Johnson, *Matrix Analysis*. Cambridge, U.K.: Cambridge Univ. Press, 2012.
[128] Y. Qin and L.-L. Yang, "Steady-state throughput analysis of network coding nodes employing stop-and-wait automatic repeat reQuest," *IEEE/ACM Trans. Netw.*, vol. 20, no. 5, pp. 1402–1411, Oct. 2012.

**ATEEQ UR REHMAN** received the B.Eng. degree in computer science and information technology from the Islamic University of Technology (OIC), Dhaka, Bangladesh, in 2009. He is currently pursuing the Ph.D. degree in wireless communications with the University of Southampton under the supervision of Prof. L.-L. Yang and Prof. L. Hanzo. He joined the Department of Computer Science, Abdul Wali Khan University Mardan, Pakistan, as a Lecturer. His main research interests are next generation wireless communications and cognitive radio networks, particularly cross layer approach and Hybrid ARQ.

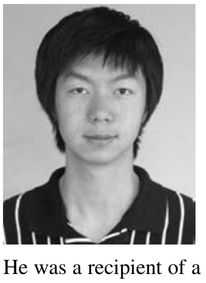

**CHEN DONG** received the B.S. degree in electronic information sciences and technology from the University of Science and Technology of China, Hefei, China, in 2004, the M.Eng. degree in pattern recognition and automatic equipment from the University of Chinese Academy of Sciences, Beijing, China, in 2007, and the Ph.D. degree from the University of Southampton, U.K., in 2014. He currently holds a post-doctoral position with the University of Southampton. He was a recipient of a Scholarship under the U.K.–China Scholarships for Excellence Programme and a Best Paper Award at the IEEE VTC 2014. His research interests include applied math, relay system, channel modeling, and cross-layer optimization.

**VARGHESE ANTONY THOMAS** received the B.E. degree (Hons.) in electrical and electronics engineering from the Birla Institute of Technology and Science, Pilani (Goa Campus), in 2010, the M.Sc. degree in wireless communications from the University of Southampton, U.K., in 2011, and the Ph.D. degree from the wireless Communications Research Group, University of Southampton, in 2015. He is currently a research associate at Georgia Institute of Technology, USA. His research interests are mainly in optical communications, optical-wireless integration, backhaul for MIMO, and radio over fiber systems. He was a recipient of the several academic awards, including the Commonwealth Scholarship of the Government of U.K. and the Mayflower Scholarship of the University of Southampton.

**LIE-LIANG YANG** (M'98–SM'02–F'16) received the B.Eng. degree in communications engineering from Shanghai Tiedao University, Shanghai, China, in 1988, and the M.Eng. and Ph.D. degrees in communications and electronics from Beijing Jiaotong University, Beijing, China, in 1991 and 1997, respectively. From 1997 to 1997, he was a Visiting Scientist with the Institute of Radio Engineering and Electronics, Czech Academy of Sciences, Prague, Czech Republic. Since 1997, he has been with the University of Southampton, Southampton, U.K., where he is currently a Professor of Wireless Communications with the School of Electronics and Computer Science. His research interest lies in wireless communications, wireless networks, and signal processing for wireless communications, and molecular and nano communications. He has authored over 300 research papers in journals and conference proceedings. He has also authored/co-authored three books and published several book chapters.

Dr. Yang is a Fellow of The Institution of Engineering and Technology, U.K. He served as an Associate Editor of the IEEE Transactions on Vehicular Technology and the *Journal of Communications and Networks*.He is currently an Associate Editor of the IEEE Access and the *Security and Communication Networks Journal*.

**LAJOS HANZO** (F'04) received the D.Sc. degree in electronics in 1976 and the Ph.D. degree in 1983. During his 40-year career in telecommunications he has held various research and academic posts in Hungary, Germany, and U.K. Since 1986, he has been with the School of Electronics and Computer Science, University of Southampton, U.K, where he holds the Chair in telecommunications. He has successfully supervised 111 Ph.D. students. He has co-authored 20 John Wiley/IEEE Press books on mobile radio communications totalling in excess of 10/,000 pages. He has published 1600+ research contributions at the IEEE Xplore and has an H-index of 62. In 2009, he received the honorary doctorate Doctor Honoris Causa by the Technical University of Budapest and in 2015 by The University of Edinburgh. He acted both as a TPC and the General Chair of IEEE conferences, presented keynote lectures, and has been awarded a number of distinctions. He is directing a 60-strong academic research team, working on a range of research projects in the field of wireless multimedia communications sponsored by industry, the Engineering and Physical Sciences Research Council, U.K., the European IST Programme, and the Mobile Virtual Centre of Excellence, U.K. He is FREng and FIET. He is an enthusiastic supporter of industrial and academic liaison and he offers a range of industrial courses. He is also a Governor of the IEEE VTS. From 2008 to 2012, he was the Editor-in-Chief of the IEEE Press and a Chaired Professor at Tsinghua University, Beijing. His research is funded by the European Research Council's Senior Research Fellow Grant.